Journal of Theoretical Biology 461 (2019) 17–33

Contents lists available at ScienceDirect

Journal of Theoretical Biology

journal homepage: www.elsevier.com/locate/jtb

Rheumatoid arthritis - a mathematical model

Nicolae Moise[a], Avner Friedman[b,*]

[a] Carol Davila University of Medicine and Pharmacy, Bucharest, Romania
[b] Mathematical Biosciences Institute & Department of Mathematics, Ohio State University, Columbus, OH, USA

ARTICLE INFO

Article history:
Received 18 April 2018
Revised 17 September 2018
Accepted 18 October 2018
Available online 19 October 2018

ABSTRACT

Rheumatoid arthritis (RA) is a common autoimmune disease that mainly affects the joints. It is characterized by synovial inflammation, which may result in cartilage and bone destruction. The present paper develops a mathematical model of chronic RA. The model is represented by a system of partial differential equations (PDEs) in the synovial fluid, the synovial membrane, and the cartilage. The model characterizes the progression of the disease in terms of the degradation of the cartilage. More precisely, we assume a simplified geometry in which the synovial membrane and the cartilage are planar layers adjacent to each other. We then quantify the state of the disease by how much the cartilage layer has decreased, or, equivalently, how much the synovial layer has increased. The model is used to evaluate treatments of RA by currently used drugs, as well as by experimental drugs.

1. Introduction

Rheumatoid Arthritis (RA) is a common autoimmune disease that affects the joints. It is characterized by synovial inflammation which ultimately leads to cartilage and bone destruction. B cells play a central role in the pathophysiology of the disease by acting as antigen presenting cells to stimulate T cells (Bugatti et al., 2014). As the disease progresses, the B cells contribute to the local synthesis of cytokines, TNF-α and IL-23 which, in turn, leads to the activation of Th-17 T cells. In the present paper we focus on the chronic state of RA, where the cells most involved in the synovial membrane are Th-17 cells, fibroblasts and inflammatory macrophages; therefore B cells will not be introduced in the mathematical model.

Th-17 cells produce IL-17 (Hashimoto, 2017; Kugyelka et al., 2016; McInnes and Schett, 2007) and GM-CSF (McInnes and Schett, 2007; Shiomi and Usui, 2015). Fibroblasts secrete IL-6 (Hashimoto, 2017; McInnes and Schett, 2007) FGF (McInnes and Schett, 2007), TNF-α (Hashimoto, 2017; McInnes and Schett, 2007), MCP-1 (Hayashida et al., 2001), and MMP (Neumann et al., 2010). Fibroblasts also produce GM-CSF, a process enhanced by TNF-α Hamilton (2008). Macrophages secrete FGF (Maruotti et al., 2013), TNF-α (Hashimoto, 2017; McInnes and Schett, 2007; Udalova et al., 2016), IL-6 (Hashimoto, 2017; McInnes and Schett, 2007), IL-23 (McInnes and Schett, 2007; Udalova et al., 2016), MMP (Kinne et al., 2007; Maruotti et al., 2013) and TIMP (Kinne et al., 2007; Maruotti et al., 2013).

On the other hand the secreted cytokines increase the activation and proliferation of the cells. Naive T cells, Th0, differentiate into Th-17 cells in the presence of TNF-α (Paradowska-Gorycka et al., 2010) and IL-6 (Hamilton, 2008; Hayashida et al., 2001; Paradowska-Gorycka et al., 2010). Macrophages are attracted to the synovial membrane by MCP-1, and the proliferation of macrophages is enhanced by GM-CSF (Hamilton, 2008; Shiomi and Usui, 2015), IL-6 (McInnes and Schett, 2007), and by contact with Th-17 in the presence of IL-23 (Kinne et al., 2007; Paradowska-Gorycka et al., 2010). Fibroblast proliferation is enhanced by TNF-α (Udalova et al., 2016), IL-17 (McInnes and Schett, 2007; Neumann et al., 2010), FGF Yuan et al. (2013), and by GM-CSF Jang et al. (2006). Finally, TIMP blocks MMP (Jang et al., 2006).

The above interactions are displayed in Fig. 1. We note that IL-1 plays an important role in RA, but since its role is similar to that of TNF-α, we did not include it in Fig. 1.

The synovial membrane lies between the synovial fluid and the cartilage. All the above cytokines, as well as MMP and TIMP, are present in the synovial fluid, but the cells remain in the synovial membrane.

The articular cartilage is a highly specialized connective tissue, whose function is to provide a smooth lubricated surface that facilitates the transmission of loads with low friction coefficients. The only cells in the cartilage are the chondrocytes. They maintain the extracellular matrix (ECM) by producing collagens. They also secrete proteoglycans that allow the connective tissue of the ECM to withstand compressional forces. In RA the number chon-

* Corresponding author.
E-mail addresses: nick.moise@gmail.com (N. Moise), afriedman@math.osu.edu (A. Friedman).

https://doi.org/10.1016/j.jtbi.2018.10.039
0022-5193/

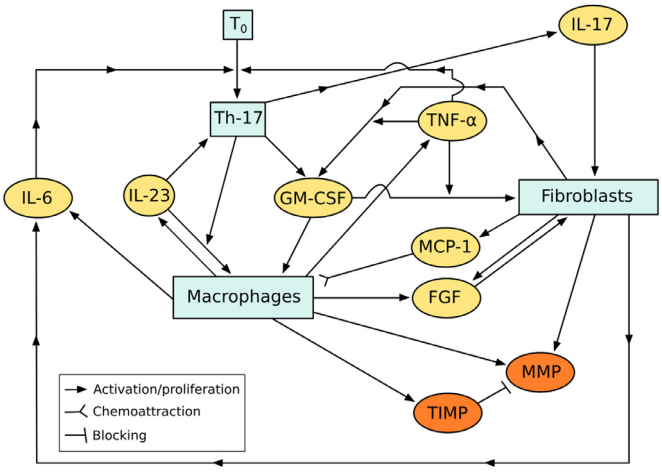

Fig. 1. Network of cells and proteins in the synovial membrane.

drocyte is decreasing as a result of the inflammation caused by TNF-α Aizawa et al. (2001), thus leading to degradation of the cartilage.

In the present paper we develop a mathematical model of RA which includes three compartments: synovial fluid, synovial membrane, and cartilage. The model equations in the synovial membrane are based on Fig. 1. We shall use the same equations, but with no cells, in the synovial fluid. In the cartilage we use the equations based on Fig. 1 but with no Th-17, macrophages and fibroblasts; instead we include chondrocytes and the ECM density.

Instead of a more realistic Fig. 2(a), we shall take the simplified geometry shown in Fig. 2(b). We note that both figures are imbedded in the 3-dimensional (x, y, z)-space. What the simplified geometry in Fig. 2.(b) means is that the dynamics of the model are independent of the variables (y, z).

Our focus in modeling the progression of RA is on the damage incurred on the articular cartilage. We measure the damage by the decrease in the thickness of the cartilage. It is known (Sakthiswary et al., 2017) that the cartilage thickness in the right knee in the control case is 2.3 mm while in RA it is 2.1 mm, and for the left knee it is 2.21 mm in the control and 2.04 mm in RA. We assume that the shrinkage in cartilage thickness is correlated with growth in the synovial membrane. Hence we take the surface of the synovial membrane, which is in contact with the cartilage, to be a time-dependent function $x = h(t)$ which is expected to increase with time as the disease progresses.

There are several mathematical models that deal with aspects of RA. Baker et al. (2013) introduced a model with inflammation (p) and anti-inflammation (a) and considered a system of two differential equations for p and a. First order kinetic saturation models of articular erosion were discussed by Witten et al. (2000). A pharmacometric model of RA, with scores as components, was described in Lacroix Lacroix (2015). In Jit et al. (2004) the effectiveness of TNF-α blockade was compared in the case of equilibrium vs. non-equilibrium of systemic response syndrome.

2. Mathematical model

The variables of the mathematical model are listed in Table 1.

We include in the model equations the treatment of RA by three drugs: infliximab (A), which blocks TNF-α; methotrexate (Y), a drug which increases apoptosis of macrophages, and tocilizumab (Z) which blocks the receptor of IL-6. The control case is when $A = 0,\ Y = 0,\ Z = 0$

Table 1
List of all the cells,proteins and drugs in units of g/cm^3. All variables are functions of (x, t).

T_{17}: Th-17 T cells	Q: MMP
M: Macrophages	Q_r: TIMP
F: Fibroblasts	C: Chondrocytes
I_{17}: IL-17	ρ: ECM density
I_{23}: IL-23	V: velocity of chondrocytes in cm/day
T_α: TNF-α	A: Infliximab
I_6: IL-6	Y: Methotrexate
S: GM-CSF	Z: Tocilizumab
G: Fibroblast growth factor, FGF	V: Anti IL-17
P: MCP-1	W: Anti IL-23

2.1. Equations in the synovial membrane, Ω^0: $L_1 < x < h(t)$

Equation for Th-17 (T_{17}). IL-6 and TNF-α induce the differentiation of naive CD4$^+$ T cells, T0, into Th-17 cells, and IL-23 enhances the proliferation of Th-17 cells. Tocilizumab blocks the interaction of T0 with IL-6 (Okuda, 2008). Hence,

$$\frac{\partial T_{17}}{\partial t} - \delta_{17}\frac{\partial^2 T_{17}}{\partial x^2} = \lambda_{TI_{23}} T_{17}\frac{I_{23}}{K_{23}+I_{23}} + \frac{\lambda_{TI_6}}{1+Z/K_Z} T_0 \frac{I_6}{K_6+I_6} + \lambda_{TT_\alpha} T_0 \frac{T_\alpha}{K_\alpha + T_\alpha} - d_{17} T_{17} \tag{2.1}$$

where T_0 is the density of T0 cells, δ_{17} is the dispersion (diffusion) coefficient, and d_{17} is the death rate. Here we used the Michaelis-Menten formula in all the production terms in order to account for receptor recycling time. For simplicity, here and in subsequent equations, we do not include delay effects, and sharp sensitivities as represented by Hill's dynamics.

Equation for macrophages (M). Macrophages are chemoattracted to the synovial membrane by MCP-1, and their proliferation is enhanced by GM-CSF and IL-6, as well as by IL-23 while in contact with Th-17. Their apoptosis is increased by methotrexate (Cutolo et al., 2001), while their interaction with IL-6 is blocked by tocilizumab (Okuda, 2008). We write the dynamics of M in the following form:

$$\frac{\partial M}{\partial t} - \delta_M \frac{\partial^2 M}{\partial x^2} = A_M - \frac{\partial}{\partial x}\left(M\chi \frac{\partial P}{\partial x}\right) + \lambda_{MI_{23}} M \frac{T_{17}}{K_{T_{17}}+T_{17}}\frac{I_{23}}{K_{23}+I_{23}} + \frac{\lambda_{MI_6}}{1+Z/K_Z} M \frac{I_6}{K_6+I_6} + \lambda_{MS} M \frac{S}{K_S+S} - d_M M - d_{MY} Y M \tag{2.2}$$

where χ is the chemotactic coefficient for MCP-1, A_M is a source of macrophages in the healthy state, and d_M is the death rate.

Equation for fibroblasts (F). We assume a logistic growth for fibroblasts, with carrying capacity F_0. Fibroblasts proliferation is enhanced by TNF-α, IL-17 and GM-CSF. Hence,

$$\frac{\partial F}{\partial t} - \delta_F \frac{\partial^2 F}{\partial x^2} = \lambda_F F\left(1 - \frac{F}{F_0}\right) + \lambda_{FT_\alpha} F \frac{T_\alpha}{K_\alpha + T_\alpha} + \lambda_{FI_{17}} F \frac{I_{17}}{K_{17}+I_{17}} + \lambda_{FG} F \frac{G}{K_G+G} - d_F F \tag{2.3}$$

Equations for cytokines.

IL-17 is produced by Th-17, hence

$$\frac{\partial I_{17}}{\partial t} - \delta_{I_{17}}\frac{\partial^2 I_{17}}{\partial x^2} = \lambda_{I_{17}T_{17}} T_{17} - d_{I_{17}} I_{17} \tag{2.4}$$

where $\delta_{I_{17}}$ is the diffusion coefficient and $d_{I_{17}}$ is the degradation rate.

IL-23 is secreted by macrophages, hence

$$\frac{\partial I_{23}}{\partial t} - \delta_{I_{23}}\frac{\partial^2 I_{23}}{\partial x^2} = \lambda_{I_{23}M} M - d_{I_{23}} I_{23} \tag{2.5}$$

where $\delta_{I_{23}}$ is the diffusion coefficient and $d_{I_{23}}$ is the degradation rate.

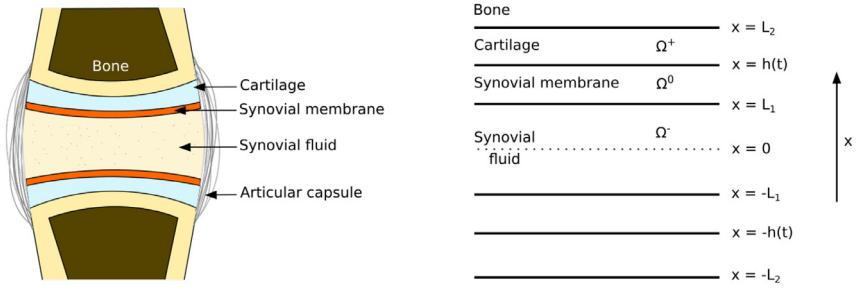

Fig. 2. (a) Normal joint anatomy. (b) Simplified geometry. The layers below $x = 0$ are a reflection of the layers above $x = 0$.

TNF-α is produced by macrophages and fibroblasts, and it is blocked by infliximab Klotz et al. (2007); Perdriger (2009). Hence TNF-α satisfies the equation

$$\frac{\partial T_\alpha}{\partial t} - \delta_{T_\alpha}\frac{\partial^2 T_\alpha}{\partial x^2} = \lambda_{T_\alpha M}M + \lambda_{T_\alpha F}F - d_{T_\alpha}T_\alpha - d_{T_\alpha A}T_\alpha A \tag{2.6}$$

where d_{T_α} is the degradation rate.

IL-6 is produced by both macrophages and fibroblasts, and its production by macrophages is inhibited by methotrexate (Cutolo et al., 2001), so that

$$\frac{\partial I_6}{\partial t} - \delta_{I_6}\frac{\partial^2 I_6}{\partial x^2} = \frac{\lambda_{I_6 M}M}{1 + Y/K_{I_6 Y}} + \lambda_{I_6 F}F - d_{I_6}I_6. \tag{2.7}$$

GM-CSF (S) is produced by Th-17. It is also produced by fibroblasts with enhancement by TNF-α. Hence,

$$\frac{\partial S}{\partial t} - \delta_S\frac{\partial^2 S}{\partial x^2} = \lambda_{ST_{17}}T_{17} + \lambda_{SF}F(1 + \lambda_{ST_\alpha}\frac{T_\alpha}{K_\alpha + T_\alpha}) - d_S S. \tag{2.8}$$

FGF (G) is produced by macrophages and fibroblasts. FGF is depleted in the process of activation of fibroblasts at a rate proportional to $F\frac{G}{K_G+G}$. The equation for FGF is as follows:

$$\frac{\partial G}{\partial t} - \delta_G\frac{\partial^2 G}{\partial x^2} = \lambda_{GM}M + \lambda_{GF}F - d_{GF}F\frac{G}{K_G + G} - d_G G. \tag{2.9}$$

MCP-1 (P) is produced by macrophages and fibroblasts, and is depleted in the process of chemoattracting macrophages at a rate proportional to $M\frac{P}{K_P+P}$. Hence P satisfies the following equation:

$$\frac{\partial P}{\partial t} - \delta_P\frac{\partial^2 P}{\partial x^2} = \lambda_{PM}M + \lambda_{PF}F - d_{PM}M\frac{P}{K_P + P} - d_P P. \tag{2.10}$$

Equations for MMP and TIMP. MMP(Q) is produced by macrophages and fibroblasts, while TIMP(Q_r) is produced by macrophages. Both MMP and TIMP are depleted at rates proportional to QQ_r when the complex MMP-TIMP is formed. The production of MMP by macrophages is lowered while the production of TIMP is enhanced by methotrexate Cutolo et al. (2001). Hence Q and Q_r satisfy the following equations:

$$\frac{\partial Q}{\partial t} - \delta_Q\frac{\partial^2 Q}{\partial x^2} = \frac{\lambda_{QM}M}{1 + Y/K_{QY}} + \lambda_{QF}F - d_{QQ_r}QQ_r - d_Q Q, \tag{2.11}$$

$$\frac{\partial Q_r}{\partial t} - \delta_{Q_r}\frac{\partial^2 Q_r}{\partial x^2} = \lambda_{Q_r M}M(1 + \gamma Y) - d_{Q_r Q}Q_r Q - d_{Q_r}Q_r. \tag{2.12}$$

Equations for drugs. For any drug X we shall denote by $I_X(t)$ the following function: $I_X(t) = 1$ if the drug is administered at time t, and $= 0$ otherwise. We denote by γ_A the effective dose rate of infliximab(A) during the dosing period, and by $\mu_{T_\alpha A}$ the depletion rate of A while blocking TNF-α. Hence,

$$\frac{\partial A}{\partial t} - \delta_A\frac{\partial^2 A}{\partial x^2} = \gamma_A I_A(t) - \mu_{T_\alpha A}T_\alpha A - d_A A. \tag{2.13}$$

We denote by γ_Y the effective dose rate of methotrexate(Y) during the dosing period, and by μ_{MY} the depletion rate of Y while interacting with macrophages. The equation for Y is thus

$$\frac{\partial Y}{\partial t} - \delta_Y\frac{\partial^2 Y}{\partial x^2} = \gamma_Y I_Y(t) - \mu_{MY}MY - d_Y Y. \tag{2.14}$$

We denote by γ_Z the effective dose rate of tocilizumab(Z) during the dosing period, and by $\mu_{I_6 Z}$ the depletion rate of Z while blocking the IL-6 receptor on T_0 and M. Hence,

$$\frac{\partial Z}{\partial t} - \delta_Z\frac{\partial^2 Z}{\partial x^2} = \gamma_Z I_Z(t) - \mu_{I_6}(T_0 + M)Z - d_Z Z \tag{2.15}$$

2.2. Equations in synovial fluid, $\Omega^-: 0 < x < L_1$

The cells (Th-17, M,F) remain in the synovial membrane, but the cytokines and the drugs can cross the permeable boundary of the synovial membrane and enter both the synovial fluid compartment, and the cartilage. We also assume that the concentration of drugs in the synovial fluid is similar to that in blood. Hence in the synovial fluid compartment Eqs. (2.4)-(2.15) hold with

$$T_{17} = 0,\ M = 0,\ F = 0.$$

2.3. Equations in cartilage, $\Omega^+: h(t) < x < L_2$

The only cells within the cartilage are chondrocytes. In healthy state there is a source A_C of chondrocytes, to replace loss due to apoptosis. However, in RA, the chondrocytes death rate is increased due to inflammation, which we take to be proportional to $C\frac{T_\alpha}{K_\alpha+T_\alpha}$. The chondrocytes produce collagen, the main component of the ECM. We denote the density of the ECM by ρ, and assume that the combined density $C + \rho$ is constant. Due to continuous remodeling of the architecture of the ECM, both ρ and C are in motion with some velocity, V.

By conservation of mass we then have

$$\frac{\partial C}{\partial t} + \frac{\partial (VC)}{\partial x} = A_C - d_{CT_\alpha}C\frac{T_\alpha}{K_\alpha + T_\alpha} - d_C C. \tag{2.16}$$

The ECM is disrupted by MMP, and we model this by a decrease in ρ at a rate proportional to ρQ. Hence, by conservation of mass,

$$\frac{\partial \rho}{\partial t} + \frac{\partial (V\rho)}{\partial x} = \lambda_{\rho C}C - d_{\rho Q}\rho Q - d_\rho \rho \tag{2.17}$$

where d_ρ is the natural degradation rate of the ECM.

Water represents 65% to 80% of the total weight of cartilage (Sophia Fox et al., 2009). We accordingly take

$$C + \rho = 0.3 g/cm^3. \tag{2.18}$$

Adding Eqs. (2.16),(2.17) we get an equation for the velocity V:

$$0.3\frac{\partial V}{\partial x} = H \tag{2.19}$$

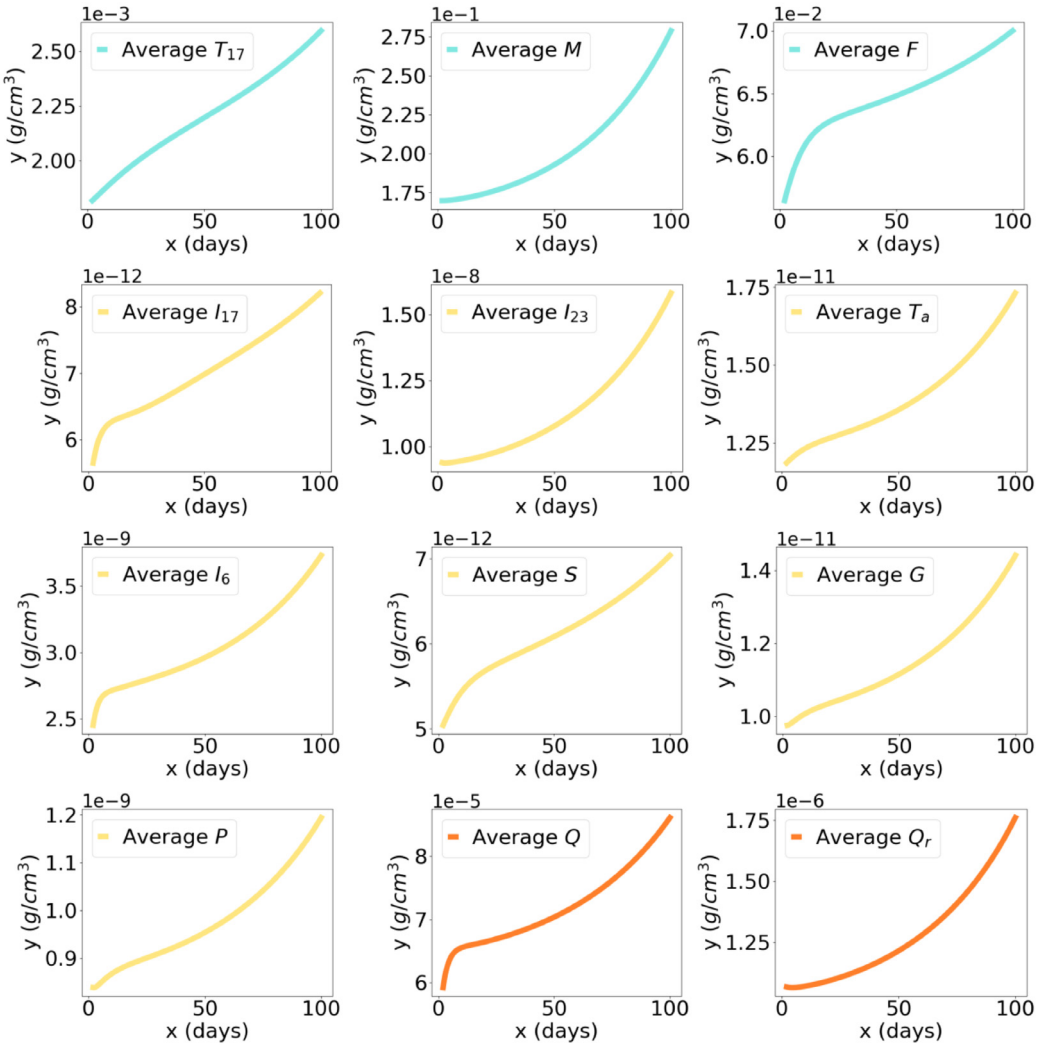

Fig. 3. Averages of cells, cytokines, MMP and TIMP over time, in domain Ω^0.

where

$$H = A_C - d_{CT_\alpha} C \frac{T_\alpha}{K_\alpha + T_\alpha} - d_C C + \lambda_{\rho C} C - d_{\rho Q} \rho Q - d_\rho \rho. \tag{2.20}$$

Assuming that $V(L_2, t) = 0$, we get

$$0.3V(x,t) = -\int_x^{L_2} H(x', t)dx' \tag{2.21}$$

and, in particular, the synovial membrane interface is moving with velocity

$$\frac{dh(t)}{dt} = V(h(t), t). \tag{2.22}$$

Eqs. (2.4), (2.5), (2.12) and (2.7)–(2.10) with $T_{17} = 0,\ M = 0,\ F = 0$ hold in the cartilage. Eqs. (2.13)–(2.15) hold with $\gamma_A = 0,\ \gamma_Y = 0,\ \gamma_Z = 0$, as we assume the cartilage is not vascularized. The equation for T_α needs to be changed to reflect a loss proportional to $C\frac{T_\alpha}{K_\alpha + T_\alpha}$:

$$\frac{\partial T_\alpha}{\partial t} - \delta_{T_\alpha} \frac{\partial^2 T_\alpha}{\partial x^2} = -d_{T_\alpha C} C \frac{T_\alpha}{K_\alpha + T_\alpha} - d_{T_\alpha} T_\alpha. \tag{2.23}$$

The equation for MMP also needs to be changed to account for the fact that chondrocytes produce MMP (Burrage et al., 2006), so that

$$\frac{\partial Q}{\partial t} - \delta_Q \frac{\partial^2 Q}{\partial x^2} = \lambda_{QC} C - d_{QQ_r} Q Q_r - d_Q Q. \tag{2.24}$$

2.4. Boundary conditions

In order to distinguish between a species X which appears in different compartments, we shall denote every species in Ω^- by X^- and every species in Ω^+ by X^+. We also denote the diffusion coefficient of species X^- (X^+) by δ_{X^-} (δ_{X^+}).

The cells T_{17}, M and F do not leave the synovial membrane, so that

$$\frac{\partial X}{\partial x} = 0 \text{ on } x = L_1 \text{ and } x = h(t), \text{ for } X = T_{17},\ M,\ F. \tag{2.25}$$

We assume that the injected drugs enter the synovial membrane through the blood, and take

$$\frac{\partial A}{\partial x} = \frac{\partial Y}{\partial x} = \frac{\partial Z}{\partial x} = 0 \text{ on } x = L_1 \text{ and } x = h(t). \tag{2.26}$$

By symmetry (see Fig. 2) we have

$$\frac{\partial X^-}{\partial x} = 0 \text{ on } x = 0 \text{ for all cytokines, MMP, TIMP and drugs.} \tag{2.27}$$

We assume that, for some $\alpha > 0$,

$$\frac{\partial X^+}{\partial x} + \alpha X^+ = 0 \text{ on } x = L_2 \text{ for all cytokines, MMP, TIMP and drugs.} \tag{2.28}$$

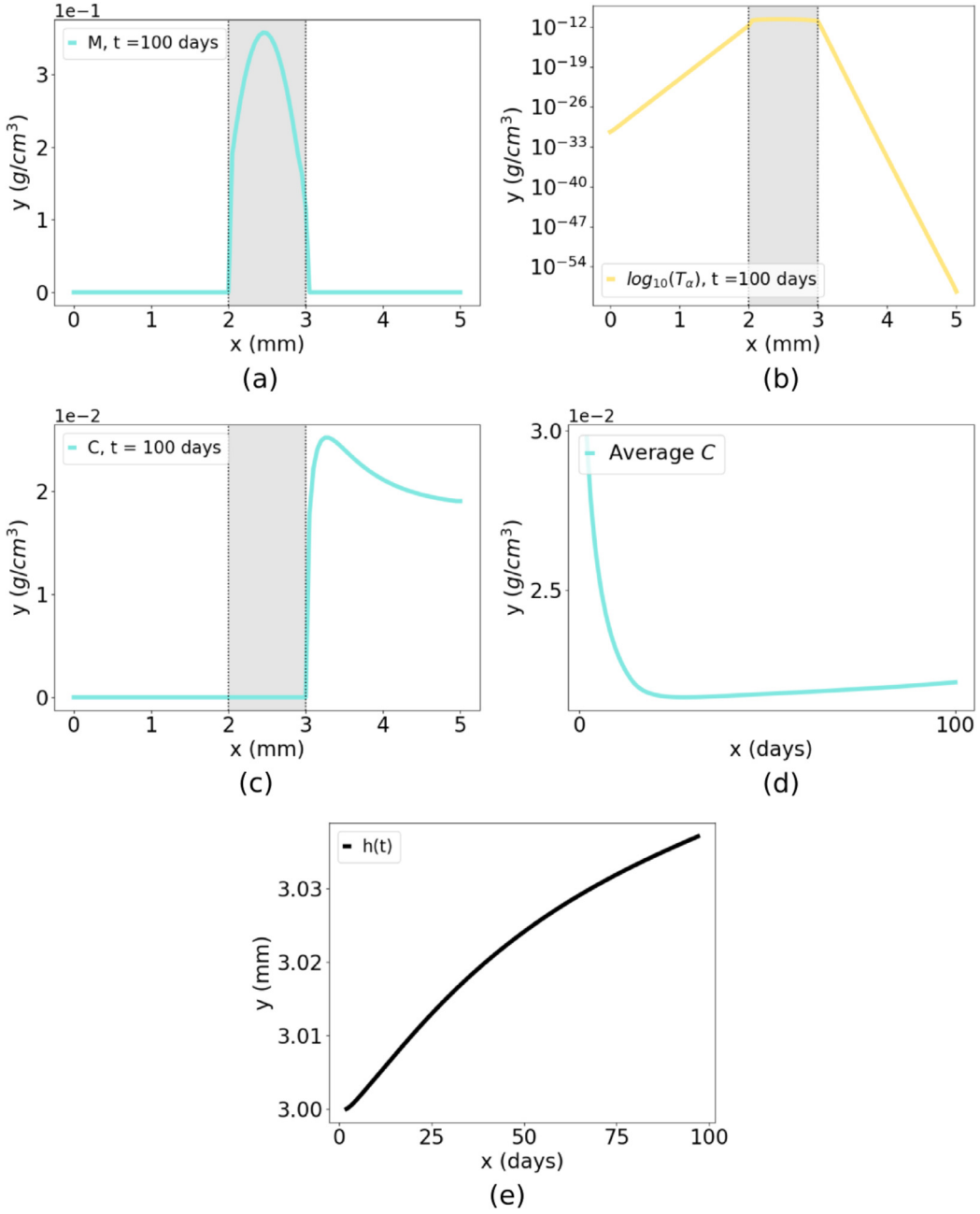

Fig. 4. (a) Profile of macrophage density. (b) Logarithmic profile of TNF-α. (c) Profile of chondrocytes. (d) Average density of chondrocytes over time. (e) Position of moving boundary $h(t)$ over time. (a),(b),(c): Domain Ω^0 in light grey.

Across the boundaries of the synovial membrane we have, by conservation of mass,

$$\delta_X \frac{\partial X}{\partial x} = \delta_{X^-} \frac{\partial X^-}{\partial x} \text{ on } x$$
$$= L_1 \text{ for all cytokines, MMP, TIMP and drugs} \quad (2.29)$$

and

$$\delta_X \frac{\partial X}{\partial x} = \delta_{X^+} \frac{\partial X^+}{\partial x} \text{ on } x$$
$$= h(t) \text{ for all cytokines, MMP, TIMP and drugs.} \quad (2.30)$$

We finally take

$$C|_{x=L} = 0.02 g/cm^3 \quad (2.31)$$

3. Results

Figs. 3and 4 are simulations of the model in the control case, i.e., when $A = Y = Z = 0$. Fig. 3 shows the profiles of the average densities/concentrations of all the species of the model in the synovial membrane during 100 days. All these averages are monotone increasing, including, in particular, the pro-inflammatory species. We assume that this is due to the progressive nature of the disease, but there are no exact quantitative data regarding the evolution of the species in time. The time-average of each species is of the same order of magnitude which was assumed in the section on parameters estimation in the appendix.

In Fig. 4 [(a), (b), (c)] we see the densities of macrophages, log-TNF-α and chondrocytes for $0 < x < 5$ (i.e., in $\Omega^- \cup \Omega^0 \cup \Omega^+$) at day 100. Macrophages are contained in the synovial membrane, as de-

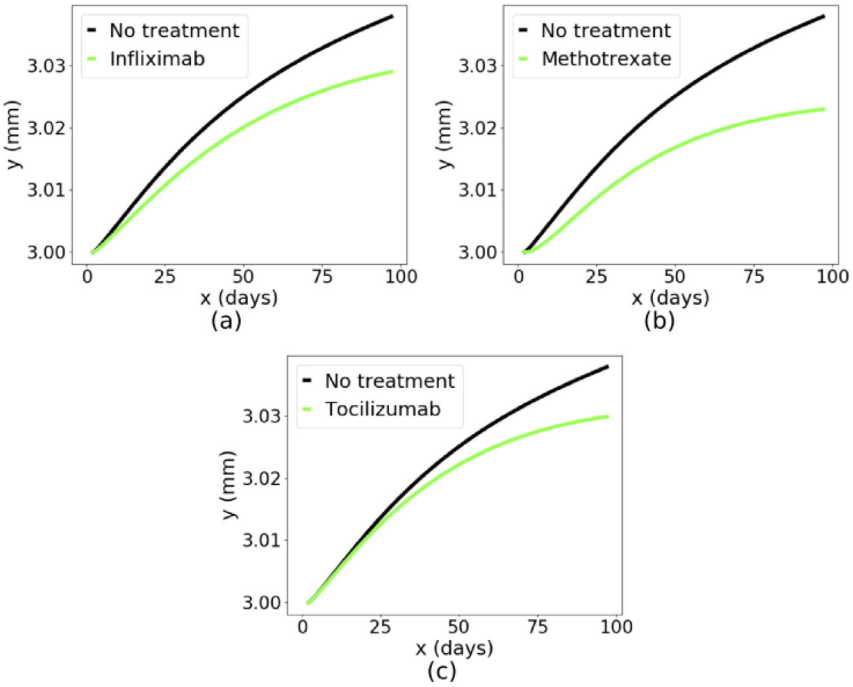

Fig. 5. Response of moving boundary h(t) to drugs.

scribed in the literature [27]. TNF-α falls very sharply from the synovial membrane into the synovial fluid and into the cartilage. This concentration of TNF-α and TNF-α producing cells in the synovial membrane is in agreement with studies that describe their distribution in the RA joint [28]. The density of chondrocytes falls sharply toward the synovial membrane, as a result of high concentration of TNF-α, but drops gradually toward the far end of the cartilage. This gradual drop may be a consequence of the relation $C + \rho = const$ (see (2.18)) and the increase in ρ due to the decrease in Q (see Eq. (2.17))

Fig. 4(d) shows the profile of the average density of the chondrocytes and Fig. 4 (e) shows the growth of h(t) during 100 days. The initial decrease in C may be the result of the choice of the initial conditions; thereafter the average density is very slightly increasing, probably because h(t) is increasing thereby decreasing the cartilage width.

As mentioned in the introduction, the cartilage in the knee of RA patients is approximately 0.18 mm thinner than normal [16]. We assume that this reduction in the cartilage occurs in a "long enough" time, which we take to be one year. The value in Fig. 4 (e) shows an increase in the thickness of the synovial membrane thickness (or decrease of cartilage) equal to approximately 0.04 mm over 100 days, which is in agreement with our assumption.

3.1. Treatment

We note that most studies of RA describe improvement, after drug administration, by clinical scores (Emery et al., 2017; Hennigan and Kavanaugh, 2008; Kaneko, 2013) (pain, number of joints affected, etc.) which are difficult to relate to cartilage thickness. Some studies use radiographic images to evaluate improvement in slowing disease progression, but they do not give exact dimensions of structure (Emery et al., 2017; Hennigan and Kavanaugh, 2008; Maini et al., 2004). In our model we view improvement by the degree to which the growth of $h(t)$ is decreased, i.e., by the degree by which the width decrease of the cartilage is slowed after treatment.

The injected level of the drug $\gamma_X (X = A, Y, Z)$ is assumed to be proportional to the dose amount injected clinically, but the proportionality parameter is unknown. We consider γ_X to be the "effective" dose for the model, and try to determine its order of magnitude by assuming that the efficacy of the drug will be between $20 - 35\%$ after 100 days. We begin with injection of only one drug, and take

$$\gamma_A = 3.45 \cdot 10^{-12} g/(cm^3 \cdot d), \ \gamma_Y = 13.85 \cdot 10^{-10} g/(cm^3 \cdot d),$$
$$\gamma_Z = 3.45 \cdot 10^{-12} g/(cm^3 \cdot d)$$

We denote by $h(t, \gamma_X)$ the profile $h(t)$ when we introduce the drug X with effective dose γ_X. Fig. 5 shows a comparison between $h(t)$ and $h(t, \gamma_X)$ for $X = A, Y, Z$. We see a reduction of $h(t)$ by $20 - 35\%$ after 100 days. We shall henceforth take the above values of γ_X as baseline for the amount of dose of the drugs.

In order to define the efficacy of a combination therapy, we define

$$h(t, \gamma_A, \gamma_Y, \gamma_Z)$$

to be the curve $h(t)$ under combined injections of $\gamma_A, \gamma_Y, \gamma_Z$ We define the efficacy of this treatment by the formula

$$E(\gamma_A, \ \gamma_Y, \ \gamma_Z) = \frac{h(100) - h(100, \gamma_A, \ \gamma_Y, \ \gamma_Z)}{h(100) - h(0)} \cdot 100\% \qquad (3.1)$$

that is, by the relative decrease of h(t).

We can use the model to compare the efficacy of different combinations. For example, by keeping γ_Y fixed, but using different amounts of γ_A and γ_Z, taking

$$((1 + \vartheta)\gamma_A, \ \gamma_Y, \ (1 - \vartheta)\gamma_Z) \text{ for } -1 < \vartheta < 1,$$

with $\gamma_A = \gamma_Z = 3.45 \cdot 10^{-12} g/(cm^3 \cdot d)$.

We set

$$E(\vartheta) = E((1 + \vartheta)\gamma_A, \ \gamma_Y, \ (1 - \vartheta)\gamma_Z)$$

Fig. 6(a) with $Y = 0$ shows that the efficacy is maximal at about 22% when $\vartheta \approx 0.1$, while Fig. 6(b) with $\gamma_Y = 13.85 \cdot 10^{-10}$ shows that the efficacy is continuously increasing when ϑ increases. This difference can be explained as follows.

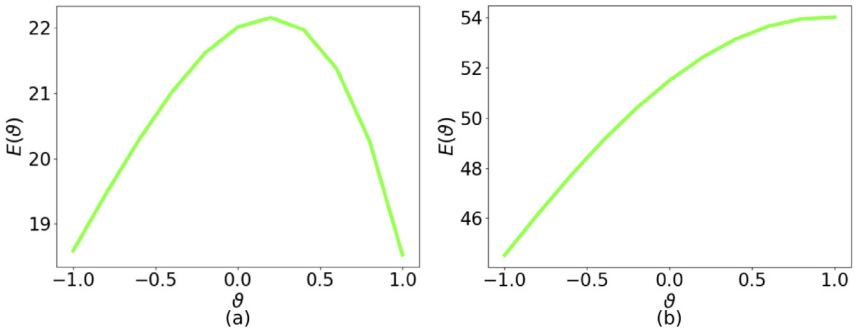

Fig. 6. Efficacy profiles for varying concentrations of A and Z with (a) $\gamma_Y = 0$ and (b) $\gamma_Y = 13.85 \cdot 10^{-10}$.

The reduction in $h(t)$ depends critically on reduction in T_α. When γ_Y increases, the density of macrophages decreases (by Eq. (2.2)) so that the additional reduction of macrophages by Z decreases. Hence the reduction in M in Eq. (2.6) is increased when γ_Y increases. On the other hand the effect of Z on F does not depend directly on the presence of Y. Hence if γ_Y is large enough, e.g. $\gamma_Y = 13.85 \cdot 10^{-10}$ the efficacy $E(\vartheta)$ is monotone increasing in ϑ for all $-1 < \vartheta < 1$

3.2. Treatment with experimental drugs

We next consider the effect of two experimental drugs, anti-IL-23 and anti-IL-17, which are used in clinical studies (Miossec, 2017; Tang et al., 2012). We take $A = Y = Z = 0$ in our model, and replace Eqs. (2.4) and (2.5) by

$$\frac{\partial I_{17}}{\partial t} - \delta_{I_{17}} \frac{\partial^2 I_{17}}{\partial x^2} = \lambda_{I_{17}T_{17}} T_{17} - d_{I_{17}} I_{17} - d_{I_{17}V} I_{17} V$$

$$\frac{\partial I_{23}}{\partial t} - \delta_{I_{23}} \frac{\partial^2 I_{23}}{\partial x^2} = \lambda_{I_{23}M} M - d_{I_{23}} I_{23} - d_{I_{23}W} I_{23} W$$

where V is anti-IL-17 and W is anti-IL-23. V and W satisfy equations similar to Eqs. (2.13), namely

$$\frac{\partial V}{\partial t} - \delta_V \frac{\partial^2 V}{\partial x^2} = \gamma_V I_V(t) - \mu_{I_{17}V} I_{17} V - d_V V.$$

$$\frac{\partial W}{\partial t} - \delta_W \frac{\partial^2 W}{\partial x^2} = \gamma_W I_W(t) - \mu_{I_{23}W} I_{23} W - d_W W.$$

Analogously to Eq. (4.1) we define the efficacy of the combination (γ_V, γ_W) by

$$E(\gamma_V\ \gamma_W) = \frac{h(100) - h(100, \gamma_V,\ \gamma_W)}{h(100) - h(0)} \cdot 100\%.$$

Fig. 7(a) is the efficacy map for a range of doses, with the color column indicating the percentage of relative decrease in the growth of the synovial membrane. The equi-efficacy curves show that the two drugs are positively correlated. With each pair (γ_V, γ_W) on an equi-efficacy curve there are associated negative side-effects. The question arises which pair will yield the least side-effects. We address this question with the example of the TNF-α: Reducing TNF-α means reducing the inflammation and its various associated negative side effects. Fig. 7(b) is a TNF-α map, showing, in the color column, the level of TNF-α average density at day 100 for each pair (γ_V, γ_W). By comparing the equi- TNF-α curves to those of the equi-efficacy curves in Fig. 7(a), we conclude that the best choice for pairs (γ_V, γ_W) in an equi-efficacy curve is the one with largest γ_W.

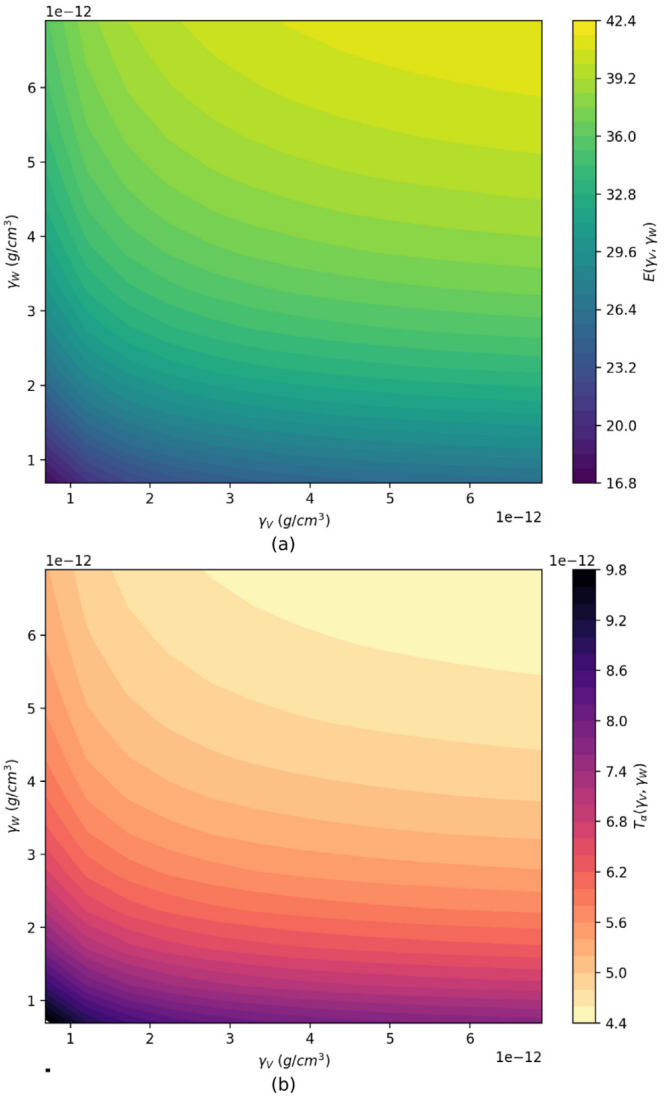

Fig. 7. (a) Efficacy map; for γ_v and γ_W in the range of $1 - 7 \cdot 10^{-12} g/cm^3 \cdot d$, the color column indicates efficacy ranging from 16.8% to 40.5%. (b) TNF-α map; the color column, for the same range of γ_V, γ_W as in Fig. 7(a), shows the average concentration of TNF-α at day 100 in the range of $4.4 \cdot 10^{-12} - 9.8 \cdot 10^{-12} g/cm^3$.

4. Conclusion

Rheumatoid arthritis (RA) is a common autoimmune disease that affects the joints. It is characterized by synovial inflammation which may result in cartilage degradation. Although the etiology of the disease is unknown, the role of excessive inflammatory

macrophages and Th-17 cells, as well as fibroblast migration and proliferation into the synovial membrane, have been documented. The present paper develops a mathematical model of chronic RA that includes, in addition to the above cells, cytokines that are produced by, or affect, the above cells, and chondrocytes that reside in the cartilage.

The clinical state of RA is currently evaluated in terms of a score (e.g. pain level, number of affected joints) or radiographic images of the degraded tissue. In the present paper we assumed a simplified geometry in which both the synovial membrane and the cartilage are taken as two planar layers adjacent to each other, and we qualified the state of the disease by how much the cartilage layer has decreased, or, equivalently, how much the adjoining synovial membrane layer expanded. We accordingly define the efficacy of a treatment by the relative decrease in the growth of the synovial membrane, $h(t)$, after $t = 100$ *days*, as compared to the control case.

The model can be used to evaluate the efficacy of any combination of drugs. For example, keeping Y (methotrexate) fixed, and varying A (infliximab) and Z (tocilizumab), by taking $(1+\vartheta)\gamma_A$ and $(1-\vartheta)\gamma_Z$, we found the efficacy increases with ϑ if γ_Y is large, but, when $\gamma_Y = 0$, it first increases and then decreases as ϑ is increased (Fig. 6).

We can also use the model to determine the efficacy of experimental drugs and, at the same time, take into account some negative side-effects. This we demonstrated in the case of V(anti IL-17) and W (anti IL-23). We showed that on any equi-efficacy curve (γ_V, γ_W) we achieve the smallest level of TNF-α by taking the largest value of γ_W on this curve.

The above two examples, and many more that can be produced by the mathematical model, must be viewed only as suggestions, or hypotheses, that need to be confirmed, or modified, when clinical data become available.

Acknowledgement

This work is supported by the Mathematical Biosciences Institute and the National Science Foundation (DMS 0931642).

Appendix. Parameter estimation

Half-saturation

In an expression of the form

$$Y\frac{X}{K_X+X}$$

where proteins X enhance the proliferation of cells Y, the parameter K_X represents the half-saturation of X. In steady state, where $X = X^0$,

$$\frac{X^0}{K_X+X^0}$$

is assumed to be not "too small" and not "too close" to 1; for simplicity we take it to be equal to 1/2 so that

$$K_X = X^0. \tag{4.1}$$

The values of X^0 will be taken from data of RA patients (see Sections 3.5, 3.6). However, in order to estimate the production parameters of cells and cytokines, we must take into account that RA is a progressive disease and, hence, in the control case (when $A = Y = Z = 0$) the densities of cells and the concentrations of cytokines, and of Q, Q_r, in the synovial membrane keep increasing in time. We shall therefore first estimate their production parameters at their steady state equations using Eq. (3.1), and then somewhat increase these parameters. The increase will be such that the "time-average" of the average concentrations taken over the synovial membrane is within order of magnitude of the values observed in RA patients. The time-average will be taken over the computational time, which we take to be 100 days.

Diffusion coefficients

In order to compute the diffusion coefficient δ_p of a protein p we use the formula Young et al. (1980)

$$\delta_p = \frac{A}{M_p^{1/3}}$$

where A is a constant and M_p is the molecular weight of p. In the special case of VEGF, we have: $M_V = 24kDa$ Hornbeck et al. (2014) and $\delta_V = 8.64\cdot 10^{-2} cm^2/d$ in tissue Liao et al. (2014). We can then compute δ_p from the list of M_p in Young et al. (1980), by the formula

$$\delta_p = \frac{M_V^{1/3}}{M_p^{1/3}}\delta_V.$$

The results are given in Table 3.

The diffusion coefficient for cells may depend on the cell type, but we assume that the differences are small, and take, as in Hao et al. (2014); Liao et al. (2014),

$$D_X = 8.64\cdot 10^{-7} cm^2/d$$

for $X = T_{17}, M$ and F.

The molecular weights of the drugs are 144 *kDa*, 454 *Da*, and 148 *kDa* for infliximab, methotrexate and tocilizumab, respectively (Wishart et al., 2017). Therefore, we obtain the following diffusion coefficients:

$$\delta_A = 4.78\cdot 10^{-2} cm^2/d$$

$$\delta_Y = 32\cdot 10^{-2} cm^2/d$$

$$\delta_Z = 4.74\cdot 10^{-2} cm^2/d$$

The diffusion of proteins and drugs in the synovial fluid is larger than in the synovial membrane, and we take

$$\delta_{p^-} = 5\delta_p.$$

On the other hand we take the diffusion of proteins in the cartilage to be the same as in the synovial membrane

$$\delta_{p^+} = \delta_p.$$

Cells death rate

We denote the half-life of species X by $t_{1/2}(X)$. Then the death/degradation rate d_X is given by the formula

$$d_X = \frac{ln2}{t_{1/2}(X)}.$$

The half-life of blood macrophages is 2 weeks, but of the Ly6C$^+$ intestinal macrophages it is 3 weeks (Italiani and Boraschi, 2014). We use the latter value because the ones in the intestinal wall are not circulating, and in a state of higher inflammatory activation, being exposed to potential pathogens in the intestines, and such reflect the ones in the inflamed synovium better. Accordingly, we get

$$d_M = \frac{ln2}{t_{1/2}(M)} = \frac{ln2}{21} = 0.33\cdot 10^{-1}/d$$

The half-life of Th-17 is 17 days (Pepper et al., 2010), hence

$$d_{T_{17}} = 0.046/d$$

The studies for fibroblasts (Nakajima et al., 1995) and chondrocytes (Kim and Song, 1999) gave the apoptosis rate as number of apoptotic cells per 100 cells (30 and 3, respectively). Taking an average apoptosis to last 24 h, we end up with a death rate of 30% and 3% of cells per day. Hence,

$$d_F = 0.3/d, \;\; d_C = 0.03/d.$$

Degradation rates

Fig. 1.A in Schwarzenberger et al. (1998) shows a decreasing profile of I_{17} with $I_{17}(3) = 110$ and $I_{17}(20) = 30$. Writing

$$\frac{dI_{17}}{dt} = -d_{I_{17}} I_{17}$$

we get, by integration,

$$30 = I_{17}(3)\exp(-17 d_{I_{17}}) = 110\exp(-17 d_{I_{17}}),$$

so that

$$d_{I_{17}} = \frac{1}{17}\ln\frac{110}{30} = 0.077/d.$$

The half-life of TNF-α is 4.6 minutes (Simó et al., 2012). Hence,

$$d_{T_\alpha} = \frac{ln2}{4.6}\cdot 24\cdot 60 = 216/d.$$

The half-life of IL-6 is 4 days (Lu et al., 1995). Hence,

$$d_{I_6} = \frac{ln2}{4} = 0.172/d.$$

The half-life of IL-23 is estimated to be 8 hours (Balestrino, 2009). Hence,

$$d_{I_{23}} = \frac{ln2}{8}\cdot 24 = 2.079/d.$$

The half-life of GM-CSF is 7 hours (Burgess and Metcalf, 1977; Tanimoto et al., 2008). Hence,

$$d_S = \frac{ln2}{7}\cdot 24 = 2.37/d.$$

The half-life of FGF varies from 4h to 13h (Shiba et al., 2003). Taking it to be 10 hours, we get

$$d_G = \frac{ln2}{10}\cdot 24 = 1.656/d.$$

The half-life of MCP-1 mRNA is around 12 hours (Safronova et al., 2003). Accordingly we take

$$d_P = 1.38/d.$$

The MMP (Q) in RA are primarily MMP-1, produced by synovial cells, and MMP-13, produced by chondrocytes (Burrage et al., 2006). The half-life of MMP-1 is 210h and of MMP-13 is 4 hours (Urbach et al., 2015). We take the half-life of MMP to be 120 hours, so that

$$d_Q = 0.138/d.$$

Based on Doherty et al. (2016), we take the half-life of TIMP to be 3.6h, so that

$$d_{Q_r} = \frac{ln2}{3.6}\cdot 24 = 4.62/d.$$

We take from Hao et al. (2017),

$$d_\rho = 0.37/d.$$

The half-life of infliximab is between 7 and 12 days (Klotz et al., 2007). Taking an average of 10 days, we get

$$d_A = 0.069/d.$$

The half-life of methotrexate is 5–8 hours (Bannwarth et al., 1996). Taking a value of 6 h, the degradation rate of methotrexate is

$$d_Y = 2.77/d.$$

The half-life of tocilizumab is 10 days (Okuda, 2008). Accordingly, the degradation rate is

$$d_Z = 0.069/d.$$

Cell densities

We first estimate the number of macrophages and fibroblasts by using two types of studies available in the literature. Both use biopsies from patients suffering from RA. The first type quantifies, using a microscope, the amount of macrophages per mm^2 (Mulherin et al., 1996). The average value given here is 400 macrophages per mm^2. Taking an estimate cell thickness of $20\mu m$, we estimate the number of cells in 1 mm^3, which gives us approximately 20,000 $cells/mm^3$, or $2\cdot 10^7 cells/mm^3$.

Another type of study uses flow cytometry to quantify the percent of leukocytes and stromal cells in synovial biopsies (Van Landuyt et al., 2010). The following percents are given: 80% leukocytes, of which 70% T cells, 15% macrophages and 5% B cells, and 20% stromal cells, of which the majority are fibroblasts. This gives us 12% of macrophages out of the total number of cells, and assuming that the number of fibroblasts is approximately 1.5 times the number of macrophages we find that the number of fibroblasts is $3\cdot 10^7 cells/cm^3$.

For Th-17 cells we also used a flow cytometry study (Shahrara et al., 2008) that gives us the percent of Th-17 cells in inflamed synovial fluid to be equal to 1.5%. Considering these to be equal to the percent in the synovial membrane, we end up with $2\cdot 10^6 cells/cm^3$.

The number of chondrocytes is $1\cdot 10^7 cells/cm^3$ (Hunziker et al., 2002).

To convert the cell numbers to cell density, we note that the size of macrophages is $20\mu m$, of fibroblasts is 10–15 μm, and of lymphocytes is 6–12 μm. Assuming that the mass of a cell of size 10 μm is $10^{-9} g$ we get the following densities M^0, F^0, T^0 for macrophages, fibroblasts and Th-17:

$$M^0 = 1.6\cdot 10^{-1} g/cm^3,$$

$$F^0 = 6\cdot 10^{-2} g/cm^3,$$

$$T_{17}^0 = 2\cdot 10^{-3} g/cm^3.$$

Recalling that the density of chondrocytes is 2% of the density of cartilage (Sophia Fox et al., 2009), we take

$$C^0 = 0.023\ g/cm^3,$$

which is consistent with the number of $1\cdot 10^7\ cells/cm^3$.

Cytokines concentrations

In steady state in RA, the concentrations of cytokines are given as follows:

IL-17 = 10 pg/ml (Metawi et al., 2011)

IL-23 = 9000 pg/ml (Kim et al., 2006)

$TNF_\alpha = 10\ \ pg/ml$ (Manabe et al., 1999), Table 3, and (Yoshida et al., 1992)

$IL_6 = 4000\ \ pg/ml$ (Manabe et al., 1999), Table 3, and (Yoshida et al., 1992)

$GM-CSF = 5\ \ pg/ml$ (Yoshida et al., 1992)

$FGF = 10\ \ pg/ml$ (Manabe et al., 1999) , Table 3

$MCP-1 = 900\ pg/ml$ (Stankovic et al., 2009)
$MMP = 10^8\ pg/ml$ (Yoshihara et al., 2000)
$TIMP = 10^6\ pg/ml$ (Yoshihara et al., 2000)

Remaining parameters

To estimate the remaining parameters in the control case we assume that the average density and concentration of each species tends to a steady state when $A = Y = Z = 0$. But, as explained in Section 3.1, all the production terms need to be increased somewhat, and these increased values are the parameter values which are listed in Table 3.

Eq. (2.1)

In the absence of data we assume that each of the three production terms contributes equally to the growth of T_{17}. We also take

$$T_0 = \frac{1}{10}T_{17}^0 = 2\cdot 10^{-4} g/cm^3.$$

Hence, in steady state,

$$\lambda_{TI_{23}} T_{17}^0 \frac{1}{2} = \lambda_{TI_6}\frac{1}{10}T_{17}^0\frac{1}{2} = \lambda_{TT_\alpha}\frac{1}{10}T_{17}^0\frac{1}{2}$$

and

$$3\lambda_{I_{23}} T_{17}^0 \frac{1}{2} = d_{T_{17}} T_{17}^0.$$

We get

$$\lambda_{I_{23}} = \frac{2}{3}d_{T_{17}} = \frac{2}{3}\cdot 0.046 = 0.0307/d,$$

$$\lambda_{TI_6} = \lambda_{TT_\alpha} = 10\cdot 0.0306 = 0.307/d.$$

Eq. (2.2)

We assume that in a healthy, normal synovial membrane the density of macrophages, M_0, is small, taking $M_0 = 10^{-5} g/m^3$. From

$$A_M - d_M M_0 = 0$$

we get

$$A_M = 0.33\cdot 10^{-1}\cdot 10^{-5} = 0.33\cdot 10^{-6} g/(cm^3\cdot d).$$

In the absence of data we take the production terms in Eq. (2.2) to be equal, so that in steady state,

$$\lambda_{MI_{23}} M^0 \frac{1}{2}\frac{1}{2} = \lambda_{MI_6} M^0 \frac{1}{2} = \lambda_{MS} M^0 \frac{1}{2}.$$

If we ignore the chemotactic term, then in steady state,

$$A_M + \frac{3}{2}\lambda_{MI_6} M^0 = d_M M^0 = 0.33\cdot 10^{-1} M^0.$$

We may ignore A_M and thus take

$$\lambda_{MI_6} = \frac{2}{3}\cdot 0.33\cdot 10^{-1} = 0.22\cdot 10^{-1}/d$$

and then

$$\lambda_{MS} = 0.22\cdot 10^{-1}/d,$$

$$\lambda_{MI_{23}} = 0.44\cdot 10^{-1}/d.$$

The parameter χ is unknown, its range could vary by several orders of magnitude. We take

$$\chi = 1000\ cm^3/g\cdot d.$$

Eq. (2.3)

Recalling that $F^0 = 6\cdot 10^{-2} g/cm^3$, we take the carrying capacity of fibroblasts to be $F_0 = 1.2\cdot 10^{-1} g/cm^3$, so that in steady state

$$1 - \frac{F}{F_0} = \frac{1}{2}.$$

We assume that production of F by I_{17} is 1.5 times larger than by T_α and 3 time larger than by G, so that in steady state,

$$\lambda_{FI_{17}} = 1.5\lambda_{FT_\alpha} = 3\lambda_{FG}.$$

From the steady state equation for F we get

$$\lambda_F\frac{1}{2} + \frac{6}{2}\lambda_{FG} = d_F = 0.3/d.$$

We assume that in a healthy case $F = \frac{1}{10}F_0 = 1.2\cdot 10^{-2} g/cm^3$, so that

$$\lambda_F(1 - \frac{1}{10}) = d_F.$$

Hence

$$\lambda_F = \frac{10}{9}d_F = \frac{10}{9}\cdot 0.3 = 0.33/d$$

and

$$\lambda_{FG} = \frac{1}{6}(0.6 - 0.33) = 0.045/d.$$

Therefore,

$$\lambda_{FT_\alpha} = 2\lambda_{FG} = 0.09/d$$

and

$$\lambda_{FT_{17}} = 3\lambda_{FG} = 0.135/d.$$

Eq. (2.4)

In steady state

$$\lambda_{I_{17}T_{17}} = \frac{d_{I_{17}}\cdot I_{17}^0}{T_{17}^0} = \frac{0.077\cdot 10^{-11}}{2\cdot 10^{-3}} = 3.85\cdot 10^{-10}/d.$$

Eq. (2.5)

In steady state

$$\lambda_{I_{23}M} = \frac{d_{I_{23}} I_{23}^0}{M^0} = \frac{2.079\cdot 9\cdot 10^{-9}}{1.6\cdot 10^{-1}} = 1.169\cdot 10^{-7}/d.$$

Eq. (2.6)

We assume that in steady state macrophages and fibroblasts contribute equally to production of T_α. Hence

$$\lambda_{T_\alpha M} M^0 = \lambda_{T_\alpha F} F^0$$

and in steady state

$$2\lambda_{T_\alpha M} = \frac{d_{T_\alpha} T_\alpha^0}{M^0} = \frac{216\cdot 10\cdot 10^{-12}}{1.6\cdot 10^{-1}}.$$

Hence,

$$\lambda_{T_\alpha M} = 6.75\cdot 10^{-9}/d.$$

and

$$\lambda_{T_\alpha F} = 6.75\cdot 10^{-9}\frac{16}{6} = 1.8\cdot 10^{-8}/d.$$

Eq. (2.7)

We assume that in steady state

$$\lambda_{I_6 M} M^0 = \lambda_{I_6 F} F^0$$

so that

$$2\lambda_{I_6 M} = \frac{d_{I_6} I_6^0}{M_0} = \frac{0.172\cdot 4\cdot 10^{-9}}{1.6\cdot 10^{-1}}.$$

Hence

$$\lambda_{I_6 M} = 2.15\cdot 10^{-9}/d$$

and

$$\lambda_{I_6 F} = 2.15\cdot 10^{-9}\frac{M_0}{F_0} = 2.15\cdot 10^{-9}\cdot\frac{16}{6} = 5.73\cdot 10^{-9}/d.$$

Eq. (2.8)

We assume that in steady state T_α doubles the production of S by fibroblasts, taking

$$\lambda_{ST_\alpha} = 2.$$

We also assume that in steady state, Th-17 and F (without T_α) contribute equally to the production of S, so that

$$\lambda_{ST_{17}} T_{17}^0 = \lambda_{SF} F^0.$$

Hence, in steady state

$$3\lambda_{SF} F^0 - d_S S^0 = 0$$

so that

$$\lambda_{SF} = \frac{2.38 \cdot S^0}{3 \cdot F^0} = \frac{2.38}{3} \cdot \frac{5 \cdot 10^{-12}}{6 \cdot 10^{-2}} = 6.60 \cdot 10^{-11}/d$$

and

$$\lambda_{ST_{17}} = 6.60 \cdot 10^{-11} \frac{F^0}{T_{17}^0} = 1.80 \cdot 10^{-9}/d.$$

Eq. (2.9)

We assume that $d_{GF} F \frac{G}{K_G + G}$ is a fraction of $d_G G$, taking, in steady state

$$d_{GF} F^0 \frac{1}{2} = \frac{1}{10} d_G G^0.$$

Hence

$$d_{GF} = \frac{1}{5} \cdot 1.67 \frac{G^0}{F^0} = \frac{1}{5} \cdot 1.67 \cdot \frac{10^{-11}}{6 \cdot 10^{-2}} = 5.43 \cdot 10^{-11}/d.$$

We also assume that in steady state M and F contribute equally to the production of G, so that

$$\lambda_{GM} M^0 = \lambda_{GF} F^0 = \frac{1}{2} \cdot \frac{11}{10} d_G G^0.$$

Hence

$$\lambda_{GM} = \frac{11}{10 \cdot 2} \cdot \frac{1.67 \cdot 10^{-11}}{1.6 \cdot 10^{-1}} = 5.74 \cdot 10^{-11}$$

and

$$\lambda_{GF} = 5.74 \cdot 10^{-11} \frac{M_0}{F_0} = 5.74 \cdot 10^{-11} \frac{1.6}{0.6} = 15.37 \cdot 10^{-11}/d.$$

Eq. (2.10)

We assume that in steady state

$$d_{PM} M^0 \frac{1}{2} = \frac{1}{10} d_P P^0$$

so that

$$d_{PM} = \frac{2}{10} \cdot \frac{1.38 \cdot 9 \cdot 10^{-10}}{1.6 \cdot 10^{-1}} = 15.55 \cdot 10^{-10}/d.$$

We also assume that in steady state

$$\lambda_{PM} M^0 = \lambda_{PF} F^0$$

so that

$$2\lambda_{PM} M^0 = \frac{11}{10} d_P P^0.$$

Hence

$$\lambda_{PM} = \frac{11}{2} \cdot \frac{1}{10} \cdot \frac{1.38 \cdot 900}{1.6} \cdot \frac{10^{-12}}{10^{-1}} = \frac{99 \cdot 1.38}{3.2} \cdot 10^{-10} = 4.269 \cdot 10^{-9}/d$$

and

$$\lambda_{PF} = 4.269 \cdot 10^{-9} \frac{M_0}{F_0} = 4.269 \cdot 10^{-9} \frac{16}{6} = 1.138 \cdot 10^{-8}/d.$$

Eqs. (2.11)(2.12)

We assume that in steady state

$$\lambda_{QM} M^0 = \lambda_{QF} F^0$$

and that

$$d_{QQ_r} Q^0 Q_r^0 = \frac{1}{10} d_Q Q^0,$$

$$d_{Q_rQ} Q_r^0 Q^0 = \frac{1}{10} d_{Q_r} Q_r$$

so

$$d_{QQ_r} = \frac{1}{10} \frac{d_Q}{Q_r^0} = 0.138 \cdot 10^5 \frac{cm^3}{g \cdot d}, \quad d_{Q_rQ} = \frac{1}{10} \frac{d_{Q_r}}{Q^0} = 4.6 \cdot 10^3 \frac{cm^3}{g \cdot d}.$$

In steady state

$$2\lambda_{QM} M^0 = \frac{11}{10} d_Q Q^0,$$

$$\lambda_{Q_r} M^0 = \frac{11}{10} d_{Q_r} Q_r^0.$$

Which give

$$\lambda_{QM} = \frac{1}{2} \cdot \frac{11}{10} \cdot \frac{0.138 \cdot 10^8 \cdot 10^{-12}}{1.6 \cdot 10^{-1}} = 4.743 \cdot 10^{-5}/d,$$

$$\lambda_{Q_rM} = \frac{11}{10} \cdot \frac{4.6 \cdot 10^6 \cdot 10^{-12}}{1.6 \cdot 10^{-1}} = 3.162 \cdot 10^{-5}/d.$$

Then

$$\lambda_{QF} = \lambda_{QM} \frac{M^0}{F^0} = 4.743 \cdot 10^{-5} \cdot \frac{16}{6} = 12.648 \cdot 10^{-5}/d.$$

Eq. (2.13)-(2.15) We assume that 80% of A is used in blocking T_α, while the remaining 20% degrades. Hence $\mu_{T_\alpha A} T_\alpha^0 A/80\% = d_A A/20\%$. Therefore

$$\mu_{T_\alpha A} = \frac{4d_A}{T_\alpha^0} = \frac{0.276}{10^{-11}} = 2.76 \cdot 10^{10} \frac{cm^3}{g \cdot d}$$

We assume that 80% of Y is used in interacting with M, while the remaining 20% degrades. Hence $\mu_{MY} M^0 Y/80\% = d_Y Y/20\%$. Therefore

$$\mu_{MY} = \frac{4d_Y}{M^0} = \frac{11.08}{1.6 \cdot 10^{-1}} = 69.25 \frac{cm^3}{g \cdot d}$$

We assume that 80% of Z is used in blocking IL-6 receptors, while the remaining 20% degrades. Hence $\mu_{I_6}(T_0 + M)Z/80\% = d_Z Z/20\%$. Therefore, with $T_0 = 0.0002$ and M near M_0, so that $T_0 + M = 0.16$,

$$\mu_{I_6} = \frac{4d_Z}{T_0 + M} = \frac{0.276}{0.16} = 1.725 \frac{cm^3}{g \cdot d}$$

The amount of drug methotrexate (Y) given to the patient is represented by γ_Y and the apoptosis rate of macrophages to the drug is represented by d_{MY}. The quantity γ_Y is proportional to the amount of administered dose, but the proportionality coefficient is not known. The parameter d_{MY} is also unknown. We assume that the apoptosis rate due to the drug increases the natural death rate, so that

$$d_{MY} Y = \frac{1}{40} d_M.$$

Taking $Y = 10^{-10} g/cm^3$

$$d_{MY} = \frac{1}{40} \frac{0.033}{10^{-10}} = 0.825 \cdot 10^7/d$$

.

We assume that

$$d_{T_\alpha A} A = \frac{d_{T_\alpha}}{1.3}$$

and take $A = 10^{-11} g/cm^3$ so that

$$d_{T\alpha A} = \frac{217}{1.3 \cdot 10^{-11}} = 16,615 \cdot 10^{11}/d.$$

Also, taking $Z = 10^{-11} g/cm^3$, we assume that

$$K_Z = 1.25 \cdot 10^{-11}$$

Finally,

$$\gamma_A = \mu_{T_\alpha A} T_\alpha A + d_A A = 2.76 \cdot 10^{10} \cdot 10^{-11} \cdot 10^{-11} + 0.069 \cdot 10^{-11} = 3.45 \cdot 10^{-12} g/(cm^3 \cdot d),$$

$$\gamma_Y = \mu_{MY} MY + d_Y Y = 69.26 \cdot 10^{-10} \cdot 1.6 \cdot 10^{-1} + 2.77 \cdot 10^{-10} = 13.85 \cdot 10^{-10} g/(cm^3 \cdot d),$$

$$\gamma_Z = \mu_{I_6}(T_0 + M)Z + d_Z Z = 1.725 \cdot 0.16 \cdot 10^{-11} + 0.069 \cdot 10^{-11} = 3.45 \cdot 10^{-12} g/(cm^3 \cdot d).$$

Eq. (2.16)

We take in healthy steady state

$$A_C - d_C C^0 = 0$$

so that

$$A_C = 0.03 \cdot 2 \cdot 10^{-2} = 0.06 \cdot 10^{-2} g/(cm^3 \cdot d).$$

We assume that in steady state

$$d_{CT_\alpha} C \frac{T_\alpha}{K_\alpha + T_\alpha} = \frac{1}{2} d_C C$$

so that

$$\frac{1}{2} d_{CT_\alpha} = \frac{1}{2} \cdot 0.03,$$

or

$$d_{CT_\alpha} = 3 \cdot 10^{-2}$$

Eq. (2.17)

In steady state

$$\lambda_{\rho C} C^0 - d_{\rho Q} \rho^0 Q^0 - d_\rho \rho^0 = 0$$

and we assume that

$$d_{\rho Q} \rho^0 Q^0 = 1.2 \cdot d_\rho \rho^0$$

so that

$$d_{\rho Q} = 0.37 \cdot 1.2 \cdot \frac{1}{Q^0} = 0.37 \cdot 1.2 \cdot 10^4 = 4.44 \cdot 10^3 g/(cm^3 \cdot d).$$

Noting that $C + \rho = 0.3$ we get $\rho_0 = 0.3 - C^0 = 0.277$. Since

$$\lambda_{\rho C} C^0 = \frac{11}{10} d_\rho \rho^0,$$

we get

$$\lambda_{\rho C} = \frac{11}{10} \cdot \frac{0.37 \cdot 0.277}{0.02} = 5.134/d.$$

Eq. (2.26)

We take $\alpha = 1$

Experimental drugs We assume that 80% of V is used in blocking I_{17}, while the remaining 20% degrades. Hence $\mu_{I_{17}V} I_{17}^0 V/80\% = d_V V/20\%$. Therefore, with $d_V = d_Z = 0.069/day$ (Okuda, 2008),

$$\mu_{I_{17}V} = \frac{4 d_V}{I_{17}^0} = \frac{0.276}{10^{-11}} = 2.76 \cdot 10^{10} \frac{cm^3}{g \cdot d}$$

We also assume that 80% of W is used in blocking I_{23}, while the remaining 20% degrades. Hence $\mu_{I_{23}W} I_{23}^0 W/80\% = d_W W/20\%$. Therefore, with $d_W = d_Z = 0.069/day$ (Okuda, 2008),

$$\mu_{I_{23}W} = \frac{4 d_W}{I_{23}^0} = \frac{0.276}{9 \cdot 10^{-9}} = 3.06 \cdot 10^7 \frac{cm^3}{g \cdot d}$$

V and W increase the degradation rate of I_{17} and I_{23}, respectively. Therefore, we assume that

$$d_{I_{17}V} V = d_{I_{17}} \cdot 10, \quad d_{I_{23}W} W = d_{I_{23}}.$$

Taking $V = W = 10^{-11} g/cm^3$, we get

$$d_{I_{17}V} = \frac{0.077 \cdot 10}{10^{-11}} = 0.077 \cdot 10^{12}/d.$$

$$d_{I_{23}W} = \frac{2.079}{10^{-11}} = 2.079 \cdot 10^{11}/d.$$

$$\gamma_V = \mu_{I_{17}V} I_{17} V + d_V V = 2.76 \cdot 10^{10} \cdot 10^{-11} \cdot 10^{-11} + 0.069 \cdot 10^{-11} = 3.45 \cdot 10^{-12} g/(cm^3 \cdot d),$$

$$\gamma_W = \mu_{I_{23}W} I_{23} W + d_W W = 3.06 \cdot 10^7 \cdot 9 \cdot 10^{-9} \cdot 10^{-11} + 0.069 \cdot 10^{-11} = 3.44 \cdot 10^{-12} g/(cm^3 \cdot d).$$

Sensitivity analysis

We carried out a sensitivity analysis for the growth of the synovial membrane at day 100, which is equivalent to the destruction of cartilage at day 100. The parameters used are the estimated production and degradation terms. Following the method described in Marino et al. (2008), we performed a Latin hypercube sampling and generated 500 samples in order to calculate the partial ranked correlation coefficients (PRCC) and the p-values with respect to the growth of the synovial membrane at day 100. In sampling the parameters, we took the range of each parameter from half to twice their values in Table 2. The results are shown in Fig. 8. In Fig. 8 we see that the production rates of all the cells (macrophages, Th-17 and fibroblasts) and cytokines, except TIMP (Q_r), are positively correlated to the destruction of the cartilage. The production rate of macrophages and the production rates of cytokines produced by them have the largest correlation. On the other hand, the production parameter $\lambda_{\rho C}$, of ECM, is negatively correlated, since the ECM helps stabilize the cartilage. The destruction coefficient of chondrocytes, d_{CT_α}, is positively correlated, since a decrease in chondrocytes increases the destruction of the cartilage.

It is also interesting to note that the production of Q, both by macrophages and by fibroblasts is highly correlated with the destruction of cartilage. Conversely, its degradation by Q_r and the increased production of Q_r by macrophages have a protective effect on the cartilage.

Computational method

We start by discretizing the space and time dimensions, with grid size Δx for space and Δt for time. For solving the diffusion equations (Eqs. (2.1) - (2.15)) we use the Crank–Nicolson method. For X being a cell or cytokine, we have:

$$\frac{\partial X}{\partial t} - D \frac{\partial^2 X}{\partial x^2} = f(x, t, X)$$

where f is the right-hand side of the equations. Then, using the discretization scheme, we obtain

$$\frac{X_i^{t+1} - X_i^t}{\Delta t} = \frac{D}{2}\left(\frac{X_{i+1}^{t+1} - 2X_i^{t+1} + X_{i-1}^{t+1}}{\Delta x^2} + \frac{X_{i+1}^t - 2X_i^t + X_{i-1}^t}{\Delta x^2}\right) + f(i, t, X).$$

Rearranging, with the unknowns on the left, we get

$$-rX_{i-1}^{t+1} + (2 + 2r)X_i^{t+1} - rX_{i+1}^{t+1} = rX_{i-1}^t + (2 - 2r)X_i^t + rX_{i+1}^t + 2\Delta t f(i, t, X_i^t)$$

Table 2
Parameters used in the model.

Notation	Description	Value	References
δ_M	Diffusion coefficient of macrophages	$8.64 \cdot 10^{-7} cm^2/d$	Young et al. (1980)
$\delta_{T_{17}}$	Diffusion coefficient of Th-17 cells	$8.64 \cdot 10^{-7} cm^2/d$	Young et al. (1980)
δ_F	Diffusion coefficient of fibroblasts	$8.64 \cdot 10^{-7} cm^2/d$	Young et al. (1980)
$\delta_{I_{17}}$	Diffusion coefficient of IL-17	$7.44 \cdot 10^{-2} cm^2/d$	Young et al. (1980)
$\delta_{I_{23}}$	Diffusion coefficient of IL-23	$9.09 \cdot 10^{-2} cm^2/d$	Young et al. (1980)
δ_{T_α}	Diffusion coefficient of TNF-α	$8.46 \cdot 10^{-2} cm^2/d$	Young et al. (1980)
δ_{I_6}	Diffusion coefficient of IL-6	$8.63 \cdot 10^{-2} cm^2/d$	Young et al. (1980)
δ_S	Diffusion coefficient of GM-CSF	$9.82 \cdot 10^{-2} cm^2/d$	Young et al. (1980)
δ_G	Diffusion coefficient of FGF	$9.58 \cdot 10^{-2} cm^2/d$	Young et al. (1980)
δ_P	Diffusion coefficient of MCP-1	$11.2 \cdot 10^{-2} cm^2/d$	Young et al. (1980)
δ_Q	Diffusion coefficient of MMP	$6.59 \cdot 10^{-2} cm^2/d$	Young et al. (1980)
δ_A	Diffusion coefficient of infliximab	$4.78 \cdot 10^{-2} cm^2/d$	Wishart et al. (2017)
δ_Y	Diffusion coefficient of methotrexate	$32 \cdot 10^{-2} cm^2/d$	Wishart et al. (2017)
δ_Z	Diffusion coefficient of tocilizumab	$4.74 \cdot 10^{-2} cm^2/d$	Wishart et al. (2017)
δ_V	Diffusion coefficient of IL-17 inhibitor	$4.74 \cdot 10^{-2} cm^2/d$	Wishart et al. (2017)
δ_W	Diffusion coefficient of IL-23 inhibitor	$4.74 \cdot 10^{-2} cm^2/d$	Wishart et al. (2017)
d_M	Macrophage death rate	$0.33 \cdot 10^{-1}/d$	Italiani and Boraschi (2014)
$d_{T_{17}}$	Th-17 death rate	$0.046/d$	Pepper et al. (2010)
d_F	Fibroblast death rate	$0.3/d$	Nakajima et al. (1995)
d_C	Chondrocyte death rate	$0.03/d$	Kim and Song (1999)
$d_{I_{17}}$	IL-17 degradation rate	$0.076/d$	Schwarzenberger et al. (1998)
$d_{I_{23}}$	IL-23 degradation rate	$2.79/d$	Balestrino (2009)
d_{T_α}	TNF-α degradation rate	$217/d$	Simó et al. (2012)
d_{I_6}	IL-6 degradation rate	$0.17/d$	Lu et al. (1995)
d_S	GM-CSF degradation rate	$2.38/d$	Burgess and Metcalf (1977); Tanimoto et al. (2008)
d_G	FGF degradation rate	$1.67/d$	Shiba et al. (2003)
d_P	MCP-1 degradation rate	$1.38/d$	Safronova et al. (2003)
d_Q	MMP degradation rate	$0.138/d$	Urbach et al. (2015)
d_{Q_r}	TIMP degradation rate	$4.62/d$	Doherty et al. (2016)
d_ρ	Cartilage ECM degradation rate	$0.37/d$	Hao et al. (2017)
d_A	Infliximab degradation rate	$0.069/d$	Klotz et al. (2007)
d_Y	Methotrexate degradation rate	$2.77/d$	Bannwarth et al. (1996)
d_Z	Tocilizumab degradation rate	$0.069/d$	Okuda (2008)
d_V	IL-17 inhibitor degradation rate	$0.069/d$	estimated
d_W	IL-23 inhibitor degradation rate	$0.069/d$	estimated
M^0	Initial density of macrophages	$1.7 \cdot 10^{-1} g/cm^3$	Mulherin et al. (1996), estimated
F^0	Initial density of fibroblasts	$5.5 \cdot 10^{-2} g/cm^3$	Van Landuyt et al. (2010), estimated
T_{17}^0	Initial density of Th-17	$1.8 \cdot 10^{-3} g/cm^3$	Shahrara et al. (2008), estimated
C^0	Initial density of chondrocytes	$0.04\, g/cm^3$	Hunziker et al. (2002); Sophia Fox et al. (2009), estimated
I_{17}^0	Initial concentration of IL-17	$5 \cdot 10^{-12} g/cm^3$	Metawi et al. (2011), estimated
I_{23}^0	Initial concentration of IL-23	$8 \cdot 10^{-9} g/cm^3$	Kim et al. (2006), estimated
T_α^0	Initial concentration of TNF-α	$1.165 \cdot 10^{-11} g/cm^3$	Manabe et al. (1999); Yoshida et al. (1992), estimated
I_6^0	Initial concentration of IL-6	$2 \cdot 10^{-9} g/cm^3$	Manabe et al. (1999); Yoshida et al. (1992), estimated
S^0	Initial concentration of GM-CSF	$3.5 \cdot 10^{-12} g/cm^3$	Yoshida et al. (1992), estimated
G^0	Initial concentration of FGF	$0.8 \cdot 10^{-11} g/cm^3$	Manabe et al. (1999), estimated
P^0	Initial concentration of MCP-1	$7 \cdot 10^{-10} g/cm^3$	Stankovic et al. (2009), estimated
Q^0	Initial concentration of MMP	$0.5 \cdot 10^{-4} g/cm^3$	Yoshihara et al. (2000), estimated
Q_r^0	Initial concentration of TIMP	$0.06 \cdot 10^{-6} g/cm^3$	Yoshihara et al. (2000), estimated
$\lambda_{I_{23}}$	Proliferation of Th-17 due to by IL-23	$0.0336/d$	estimated*
λ_{TI_6}	Proliferation of Th-17 due to by IL-6	$0.336/d$	estimated*
λ_{TT_α}	Proliferation of Th-17 due to TNF-α	$0.336/d$	estimated*
A_M	Basal influx of macrophages	$0.33 \cdot 10^{-6} g/(cm^3 \cdot d)$	estimated
λ_{MI_6}	Proliferation of macrophages due to IL-6	$0.242 \cdot 10^{-1}/d$	estimated*
λ_{MS}	Proliferation of macrophages due to GM-CSF	$0.242 \cdot 10^{-1}/d$	estimated*
$\lambda_{MI_{23}}$	Proliferation of macrophages due to IL-23	$0.484 \cdot 10^{-1}/d$	estimated*
d_{MY}	Depletion of macrophages due to methotrexate	$3.3 \cdot 10^{-1}/d$	estimated
χ	Chemotactic coefficient	$1000\, cm^3/(g \cdot d)$	estimated*
F_0	Fibroblast carrying capacity	$1.2 \cdot 10^{-1} g/cm^3$	estimated
λ_F	Basal proliferation of fibroblasts	$0.33/d$	estimated*
λ_{FT_α}	Proliferation of fibroblasts due to TNF-α	$0.099/d$	estimated*
$\lambda_{FI_{17}}$	Proliferation of fibroblasts due to IL-17	$0.148/d$	estimated*
λ_{FG}	Proliferation of fibroblasts due to FGF	$0.0495/d$	estimated*
$\lambda_{I_{17}T_{17}}$	Production of IL-17 by Th-17	$5.39 \cdot 10^{-10}/d$	estimated*
$d_{I_{17}V}$	Depletion of IL-17 by IL-17 inhibitor	$0.077 \cdot 10^{12}/d$	estimated
$\lambda_{I_{23}M}$	Production of IL-23 by macrophages	$1.402 \cdot 10^{-7}/d$	estimated*
$d_{I_{23}W}$	Depletion of IL-23 by IL-23 inhibitor	$2.079 \cdot 10^{11}/d$	estimated

(*continued on next page*)

Table 2 (*continued*)

Notation	Description	Value	References
$\lambda_{T_\alpha M}$	Production of TNF-α by macrophages	$8.1 \cdot 10^{-9}/d$	estimated*
$\lambda_{T_\alpha F}$	Production of TNF-α by fibroblasts	$2.16 \cdot 10^{-8}/d$	estimated*
$d_{T_\alpha A}$	Depletion of TNF-α by infliximab	$166.15 \cdot 10^{11}/d$	estimated
$\lambda_{I_6 M}$	Production of IL-6 by macrophages	$2.58 \cdot 10^{-9}/d$	estimated*
$\lambda_{I_6 F}$	Production of IL-6 by fibroblasts	$6.876 \cdot 10^{-9}/d$	estimated*
$K_{I_6 Y}$	Inhibition of macrophage IL-6 production by methotrexate	$1.25 \cdot 10^{-10} g/cm^3$	estimated
K_Z	Half-saturation of tocilizumab at the IL-6 receptor	$10^{-11} g/cm^3$	estimated
λ_{ST_α}	Production of GM-CSF by fibroblasts due to TNF-α	2.4	estimated*
$\lambda_{ST_{17}}$	Production of GM-CSF by Th-17	$2.368 \cdot 10^{-9}/d$	estimated*
λ_{SF}	Production of GM-CSF by fibroblasts	$7.899 \cdot 10^{-11}/d$	estimated*
d_{GF}	Depletion of FGF by internalized receptors	$5.43 \cdot 10^{-11}/d$	estimated
λ_{GM}	Production of FGF by macrophages	$6.828 \cdot 10^{-11}/d$	estimated*
λ_{GF}	Production of FGF by fibroblasts	$18.216 \cdot 10^{-11}/d$	estimated*
d_{PM}	Depletion of MCP-1 by internalized receptors	$15.55 \cdot 10^{-10}/d$	estimated
λ_{PM}	Production of MCP-1 by macrophages	$5.122 \cdot 10^{-9}/d$	estimated*
λ_{PF}	Production of MCP-1 by fibroblasts	$1.365 \cdot 10^{-8}/d$	estimated*
λ_{QM}	Production of MMP by macrophages	$5.217 \cdot 10^{-5}/d$	estimated*
λ_{QF}	Production of MMP by fibroblasts	$13.912 \cdot 10^{-5}/d$	estimated*
K_{QY}	Inhibition of macrophage MMP production by methotrexate	$10^{-10} g/cm^3$	estimated
d_{QQ_r}	Depletion of MMP by forming complexes with TIMP	$0.138 \cdot 10^5\ cm^3/(g \cdot d)$	estimated
$\lambda_{Q_r M}$	Production of TIMP by macrophages	$3.47 \cdot 10^{-5}/d$	estimated*
$d_{Q_r Q}$	Depletion of TIMP by forming complexes with MMP	$4.6 \cdot 10^3\ cm^3/(g \cdot d)$	estimated
γ_A	Infliximab effective dose rate	$3.45 \cdot 10^{-12} g/(cm^3 \cdot d)$	estimated
γ_Y	Methotrexate effective dose rate	$13.85 \cdot 10^{-10} g/(cm^3 \cdot d)$	estimated
γ_Z	Tocilizumab effective dose rate	$3.45 \cdot 10^{-12} g/(cm^3 \cdot d)$	estimated
γ_V	IL-17 inhibitor effective dose rate	$3.45 \cdot 10^{-12} g/(cm^3 \cdot d)$	estimated
γ_W	IL-23 inhibitor effective dose rate	$3.44 \cdot 10^{-12} g/(cm^3 \cdot d)$	estimated
$\mu_{T_\alpha A}$	Degradation rate of infliximab while blocking TNF-α	$2.76 \cdot 10^{10} g/(cm^3 \cdot d)$	estimated
μ_{MY}	Degradation rate of methotrexate from macrophage interactions	$69.25 g/(cm^3 \cdot d)$	estimated
μ_{I_6}	Degradation rate of tocilizumab while interacting with the IL-6 receptor	$1.725 g/(cm^3 \cdot d)$	estimated
$\mu_{I_{17}V}$	Degradation rate of IL-17 inhibitor while blocking IL-17	$2.76 \cdot 10^{10} g/(cm^3 \cdot d)$	estimated
$\mu_{I_{23}W}$	Degradation rate of IL-23 inhibitor while blocking IL-23	$3.06 \cdot 10^7 g/(cm^3 \cdot d)$	estimated
A_C	Basal proliferation of chondrocytes	$6 \cdot 10^{-4}\ g/(cm^3 \cdot d)$	estimated
d_{CT_α}	Apoptosis of chondrocytes due to TNF-α	$3 \cdot 10^{-2}$	estimated
$\lambda_{\rho C}$	Production of ECM by chondrocytes	$5.698/d$	estimated*
$d_{\rho Q}$	Degradation of cartilage ECM by MMP	$4.44 \cdot 10^3 g/(cm^3 \cdot d)$	estimated

* the value is somewhat larger than the value estimated in Section 3.7 (as explained in the section "Half-saturation" of the "Parameters estimation" in Appendix.)

Table 3
Diffusion coefficients of proteins p in the synovial membrane. M_p in units of kDa and δ_p in units of $10^{-2} cm^2/d$.

P	I_{17}	I_{23}	T_α	I_6	$GM-CSF$	FGF	$MCP-1$	MMP	$TIMP$
M_p	37.5	20.7	25.6	23.7	16.3	17.6	11	54	24
δ_p	7.44	9.09	8.46	8.63	9.82	9.58	11.2	6.59	8.64

where

$$r = D\frac{\Delta t}{\Delta x^2}.$$

Applying this to each point of the space domain at a certain time t, we obtain a system of N equations with N unknowns. By solving this system, we obtain the values for the next time-step, $t+1$.

Boundary conditions for cells

The boundaries of the domain are not explicitly used in the Crank–Nicolson method. Instead, suppose there is an X_0 at $x = L_1$, just outside our scheme. Re-writing the scheme at $x = L_1 + \Delta x$, we get:

$$-rX_0^{t+1} + (2+2r)X_1^{t+1} - rX_2^{t+1} = rX_0^t + (2-2r)X_1^t + rX_2^t + 2\Delta t f(L_1, t, X_1^t).$$

We thus have one too many unknowns for our system of equations. But from our boundary conditions

$$\frac{X_1 - X_0}{\Delta x} = 0$$

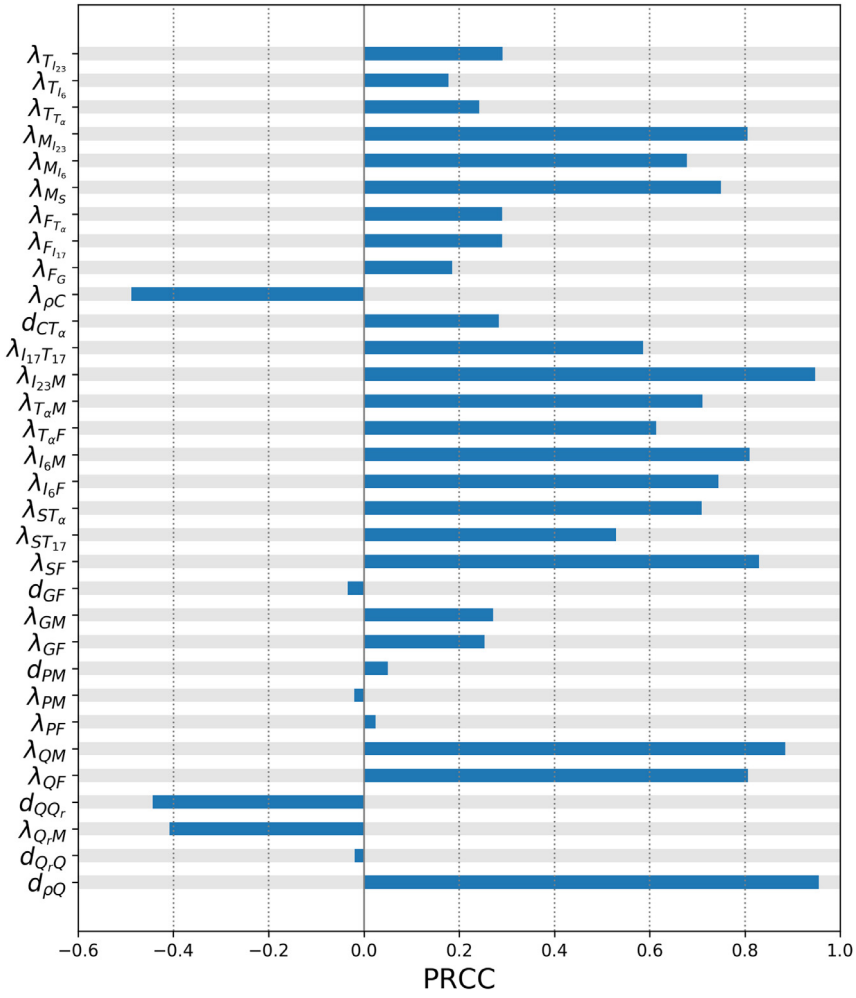

Fig. 8. PRCC values for synovial membrane growth at day 100. All values are statistically significant ($p < .01$).

so that

$$X_1 = X_0.$$

Therefore,

$$-rX_1^{t+1} + (2+2r)X_1^{t+1} - rX_2^{t+1} = rX_1^t + (2-2r)X_1^t + rX_2^t + 2\Delta t f(L_1, t, X_1^t).$$

At the moving boundary we suppose there is a point at position $h(t)$, for which we interpolate the value, as described in D'Acunto (2004). We use this value in the scheme above. Writing the scheme at the boundary, we get:

$$-rX_{i-2}^{t+1} + (2+2r)X_{i-1}^{t+1} - rX_i^{t+1} = rX_{i-2}^t + (2-2r)X_{i-1}^t + rX_i^t + 2\Delta t f(i-1, t, X_{i-1}^t).$$

Having one extra unknown, X_i^{t+1}, we need to write it in terms of known grid points. We know that, by discretizing,

$$\frac{X_i^{t+1} - X_i^t}{\Delta t} = D\frac{\partial^2 x}{\partial x^2}|_{t,i} + f|_{t,i}$$

We then write the space derivative using interpolation. Thus:

$$X_i^{t+1} = X_i^t + D\Delta t \frac{2}{\Delta x^2}\left(\frac{X_{i-1}^t}{1+p} - \frac{X_i^t}{p} + \frac{X_p^t}{p(1+p)}\right) + \Delta t f|_{t,i}$$

where $p = h(t) - i\Delta x$, the distance from the nearest fixed grid point.

But since X_p^t is the boundary, and $\frac{\partial X(h(t))}{\partial x} = 0$, we get

$$\frac{X_p^t - X_i^t}{p} = 0$$

thus

$$X_p^t = X_i^t.$$

Substituting X_i^{t+1}, we have:

$$\begin{aligned} - \quad & rX_{i-2}^{t+1} + (2+2r)X_{i-1}^{t+1} - r[X_i^t + 2r(\tfrac{X_{i-1}^t}{1+p} - \tfrac{X_i^t}{p} + \tfrac{X_i^t}{p(1+p)}) + \Delta t f(i,t,X_i^t)] \\ = \quad & rX_{i-2}^t + (2-2r)X_{i-1}^t + rX_i^t + 2\Delta t f(i-1,t,X_{i-1}^t) \end{aligned}$$

therefore

$$\begin{aligned} - \quad & rX_{i-2}^{t+1} + (2+2r)X_{i-1}^{t+1} \\ = \quad & rX_{i-2}^t + X_{i-1}^t(\tfrac{2r^2}{1+p} + 2 + 2r) + X_i^t(r + \tfrac{2r^2}{p(1+p)} - \tfrac{2r^2}{p}) \\ + \quad & r\Delta t f(i,t,X_i^t) + 2\Delta t f(i-1,t,X_{i-1}^t). \end{aligned}$$

This eliminates the extra unknown and allows us to solve the system.

Boundary conditions for cytokines

For simplicity, we use a single domain for the cytokines, taking care to use the appropriate diffusion coefficient in Ω^-. We therefore have two borders, $x = 0$ and $x = L_2$.

x = 0

The case here is the same as for the cells at $x = L_1$, described above.

$x = L_2$

At boundary L_2 we have the condition

$$\frac{\partial X}{\partial x} + \alpha X = 0.$$

Suppose there is an X_i at $x = L_2$. Writing the CN scheme at $x = L_2 - \Delta x$ we get:

$$-rX_{i-2}^{t+1} + (2+2r)X_{i-1}^{t+1} - rX_i^{t+1} = rX_{i-2}^t + (2-2r)X_{i-1}^t + rX_i^t + \Delta t f(i-1, t, X_{i-1}^t).$$

From our boundary conditions, we know, by discretizing, that

$$\frac{X_i - X_{i-1}}{\Delta x} + \alpha X_i = 0.$$

It follows that

$$X_i = \frac{X_i - 1}{1 + \alpha \Delta x}$$

We then replace X_2 in the scheme, getting

$$-rX_{i-2}^{t+1} + (2+2r - \frac{r}{1+\alpha\Delta x})X_{i-1}^{t+1} = rX_{i-2}^t + (2-2r+\frac{r}{1+\alpha\Delta x})X_{i-1}^t + \Delta t f(i-1, t, X_{i-1}^t).$$

which we can solve for the next time-level at the border.

Advection equations

For the advection equations (Eqs. (2.16), (2.17)), we use the upwind method. We first break up $\frac{\partial (VX)}{\partial x}$:

$$\frac{\partial X}{\partial t} + \frac{\partial (VX)}{\partial x} - f(x,t,X) = \frac{\partial X}{\partial t} + V\frac{\partial X}{\partial x} + X\frac{\partial V}{\partial x} - f(x,t,X) = 0.$$

But from Eq. (2.19) we know that $0.3 \cdot \frac{\partial V}{\partial x} = H$. Therefore we substitute $\frac{\partial V}{\partial x}$ with $\frac{H}{0.3}$:

$$\frac{\partial X}{\partial t} + V\frac{\partial X}{\partial x} + X\frac{H}{0.3} - f(x,t,X) = 0.$$

We then discretize this using the upwind method:

$$\frac{X_i^{t+1} - X_i^t}{\Delta t} + V(t,i)\frac{X_i^t - X_{i-1}^t}{\Delta x} + X_i^t\frac{H}{0.3} - f(i,t,X_i^t) = 0.$$

and obtain X_i^{t+1}.

References

Aizawa, T., Kon, T., Einhorn, T., Gerstenfeld, L., 2001. Induction of apoptosis in chondrocytes by tumor necrosis factor-alpha. J. Orthopaedic Res. 19 (5), 785–796.

Baker, M., Denman-Johnson, S., Brook, B.S., Gaywood, I., Owen, M.R., 2013. Mathematical modelling of cytokine-mediated inflammation in rheumatoid arthritis. Math. Med. Biol. 30 (4), 311–337.

Balestrino, M., 2009. Cytokine imbalances in multiple sclerosis: a computer simulation. Master of Engineering Projects, Cornell University.

Bannwarth, B., Péhourcq, F., Schaeverbeke, T., Dehais, J., 1996. Clinical pharmacokinetics of low-dose pulse methotrexate in rheumatoid arthritis. Clin. Pharmacokinet. 30 (3), 194–210.

Bugatti, S., Vitolo, B., Caporali, R., Montecucco, C., Manzo, A., 2014. B cells in rheumatoid arthritis: from pathogenic players to disease biomarkers. Biomed. Res. Int. 2014.

Burgess, A., Metcalf, D., 1977. Serum half-life and organ distribution of radiolabeled colony stimulating factor in mice.. Exp. Hematol. 5 (6), 456–464.

Burrage, P.S., Mix, K.S., Brinckerhoff, C.E., et al., 2006. Matrix metalloproteinases: role in arthritis. Front Biosci. 11 (1), 529–543.

Cutolo, M., Sulli, A., Pizzorni, C., Seriolo, B., Straub, R., 2001. Anti-inflammatory mechanisms of methotrexate in rheumatoid arthritis. Ann. Rheum. Dis. 60 (8), 729–735.

D'Acunto, B., 2004. Computational methods for PDE in mechanics, 67. World scientific.

Doherty, C.M., Visse, R., Dinakarpandian, D., Strickland, D.K., Nagase, H., Troeberg, L., 2016. Engineered tissue inhibitor of metalloproteinases-3 variants resistant to endocytosis have prolonged chondroprotective activity. J. Biol. Chem. 291 (42), 22160–22172.

Emery, P., Vencovskỳ, J., Sylwestrzak, A., Leszczyński, P., Porawska, W., Stasiuk, B., Hilt, J., Mosterova, Z., Cheong, S.Y., Ghil, J., 2017. Long-term efficacy and safety in patients with rheumatoid arthritis continuing on sb4 or switching from reference etanercept to sb4. Ann. Rheum. Dis.. annrheumdis–2017

Hamilton, J.A., 2008. Colony-stimulating factors in inflammation and autoimmunity. Nat. Rev. Immunol. 8 (7), 533–544.

Hao, W., Crouser, E.D., Friedman, A., 2014. Mathematical model of sarcoidosis. Proc. Natl. Academy of Sci. 111 (45), 16065–16070.

Hao, W., Komar, H.M., Hart, P.A., Conwell, D.L., Lesinski, G.B., Friedman, A., 2017. Mathematical model of chronic pancreatitis. Proc. Natl. Acad. Sci. 114 (19), 5011–5016.

Hashimoto, M., 2017. Th17 in animal models of rheumatoid arthritis. J. Clin. Med. 6 (7), 73.

Hayashida, K., Nanki, T., Girschick, H., Yavuz, S., Ochi, T., Lipsky, P.E., 2001. Synovial stromal cells from rheumatoid arthritis patients attract monocytes by producing mcp-1 and il-8. Arthritis Res. Therapy 3 (2), 118.

Hennigan, S., Kavanaugh, A., 2008. Interleukin-6 inhibitors in the treatment of rheumatoid arthritis. Ther. Clin. Risk Manag. 4 (4), 767.

Hornbeck, P.V., Zhang, B., Murray, B., Kornhauser, J.M., Latham, V., Skrzypek, E., 2014. Phosphositeplus, 2014: mutations, ptms and recalibrations. Nucleic Acids Res. 43 (D1), D512–D520.

Hunziker, E., Quinn, T., Häuselmann, H.-J., 2002. Quantitative structural organization of normal adult human articular cartilage. Osteoarthritis and Cartilage 10 (7), 564–572.

Italiani, P., Boraschi, D., 2014. From monocytes to m1/m2 macrophages: phenotypical vs. functional differentiation. Front Immunol. 5.

Jang, J., Lim, D.-S., Choi, Y.-E., Jeong, Y., Yoo, S.-A., Kim, W.-U., Bae, Y.-S., 2006. Mln51 and gm-csf involvement in the proliferation of fibroblast-like synoviocytes in the pathogenesis of rheumatoid arthritis. Arthritis Res. Therapy 8 (6), R170.

Jit, M., Henderson, B., Stevens, M., Seymour, R., 2004. Tnf-α neutralization in cytokine-driven diseases: a mathematical model to account for therapeutic success in rheumatoid arthritis but therapeutic failure in systemic inflammatory response syndrome. Rheumatology 44 (3), 323–331.

Kaneko, A., 2013. Tocilizumab in rheumatoid arthritis: efficacy, safety and its place in therapy. Ther. Adv. Chronic Dis. 4 (1), 15–21.

Kim, H.A., Song, Y.W., 1999. Apoptotic chondrocyte death in rheumatoid arthritis. Arthritis & Rheumatol. 42 (7), 1528–1537.

Kim, H.-R., Cho, M.-L., Kim, K.-W., Juhn, J.-Y., Hwang, S.-Y., Yoon, C.-H., Park, S.-H., Lee, S.-H., Kim, H.-Y., 2006. Up-regulation of il-23p19 expression in rheumatoid arthritis synovial fibroblasts by il-17 through pi3-kinase-, nf-κb-and p38 mapk-dependent signalling pathways. Rheumatology 46 (1), 57–64.

Kinne, R.W., Stuhlmüller, B., Burmester, G.-R., 2007. Cells of the synovium in rheumatoid arthritis. macrophages. Arthritis Res. Therapy 9 (6), 224.

Klotz, U., Teml, A., Schwab, M., 2007. Clinical pharmacokinetics and use of infliximab. Clin. Pharmacokinet. 46 (8), 645–660.

Kugyelka, R., Kohl, Z., Olasz, K., Mikecz, K., Rauch, T.A., Glant, T.T., Boldizsar, F., 2016. Enigma of il-17 and th17 cells in rheumatoid arthritis and in autoimmune animal models of arthritis. Mediators Inflamm. 2016.

Lacroix, B., 2015. Pharmacometric Modeling in Rheumatoid Arthritis. Acta Universitatis Upsaliensis.

Liao, K.-L., Bai, X.-F., Friedman, A., 2014. Mathematical modeling of interleukin-27 induction of anti-tumor t cells response. PLoS ONE 9 (3), e91844.

Lu, Z.Y., Brailly, H., Wijdenes, J., Bataille, R., Rossi, J., Klein, B., 1995. Measurement of whole body interleukin-6 (il-6) production: prediction of the efficacy of anti-il-6 treatments. Blood 86 (8), 3123–3131.

Maini, R., Breedveld, F., Kalden, J., Smolen, J., Furst, D., Weisman, M., St Clair, E., Keenan, G., Van Der Heijde, D., Marsters, P., et al., 2004. Sustained improvement over two years in physical function, structural damage, and signs and symptoms among patients with rheumatoid arthritis treated with infliximab and methotrexate. Arth. Rheumatol. 50 (4), 1051–1065.

Manabe, N., Oda, H., Nakamura, K., Kuga, Y., Uchida, S., Kawaguchi, H., 1999. Involvement of fibroblast growth factor-2 in joint destruction of rheumatoid arthritis patients. Rheumatology 38 (8), 714–720.

Marino, S., Hogue, I.B., Ray, C.J., Kirschner, D.E., 2008. A methodology for performing global uncertainty and sensitivity analysis in systems biology. J. Theor. Biol. 254 (1), 178–196.

Maruotti, N., Annese, T., Cantatore, F.P., Ribatti, D., 2013. Macrophages and angiogenesis in rheumatic diseases. Vascular cell 5 (1), 11.

McInnes, I.B., Schett, G., 2007. Cytokines in the pathogenesis of rheumatoid arthritis. Nat. Rev. Immunol. 7 (6), 429–442.

Metawi, S.A., Abbas, D., Kamal, M.M., Ibrahim, M.K., 2011. Serum and synovial fluid levels of interleukin-17 in correlation with disease activity in patients with ra. Clin. Rheumatol. 30 (9), 1201.

Miossec, P., 2017. Update on interleukin-17: a role in the pathogenesis of inflammatory arthritis and implication for clinical practice. RMD Open 3 (1), e000284.

Mulherin, D., Fitzgerald, O., Bresnihan, B., 1996. Synovial tissue macrophage populations and articular damage in rheumatoid arthritis. Arth. Rheumatol. 39 (1), 115–124.

Nakajima, T., Aono, H., Hasunuma, T., Yamamoto, K., Shirai, T., Hirohata, K., Nishioka, K., 1995. Apoptosis and functional fas antigen in rheumatoid arthritis synoviocytes. Arthritis Rheumatol. 38 (4), 485–491.

Neumann, E., Lefèvre, S., Zimmermann, B., Gay, S., Müller-Ladner, U., 2010. Rheumatoid arthritis progression mediated by activated synovial fibroblasts. Trends Mol. Med. 16 (10), 458–468.

Okuda, Y., 2008. Review of tocilizumab in the treatment of rheumatoid arthritis. Biologics 2 (1), 75.

Paradowska-Gorycka, A., Grzybowska-Kowalczyk, A., Wojtecka-Lukasik, E., Maslinski, S., 2010. Il-23 in the pathogenesis of rheumatoid arthritis. Scand. J. Immunol. 71 (3), 134–145.

Pepper, M., Linehan, J.L., Pagán, A.J., Zell, T., Dileepan, T., Cleary, P.P., Jenkins, M.K.,

2010. Different routes of bacterial infection induce long-lived th1 memory cells and short-lived th17 cells. Nat. Immunol. 11 (1), 83–89.
Perdriger, A., 2009. Infliximab in the treatment of rheumatoid arthritis. Biologics: Targets Therapy 3, 183.
Safronova, O., Nakahama, K., Onodera, M., Muneta, T., Morita, I., 2003. Effect of hypoxia on monocyte chemotactic protein-1 (mcp-1) gene expression induced by interleukin-1ß in human synovial fibroblasts. Inf. Res. 52 (11), 480–486.
Sakthiswary, R., Rajalingam, S., Hussein, H., Sridharan, R., Asrul, A.W., 2017. Cartilage oligomeric matrix protein (comp) in rheumatoid arthritis and its correlation with sonographic knee cartilage thickness and disease activity. Clin. Rheumatol. 1–6.
Schwarzenberger, P., La Russa, V., Miller, A., Ye, P., Huang, W., Zieske, A., Nelson, S., Bagby, G.J., Stoltz, D., Mynatt, R.L., et al., 1998. Il-17 stimulates granulopoiesis in mice: use of an alternate, novel gene therapy-derived method for in vivo evaluation of cytokines. J. Immunol. 161 (11), 6383–6389.
Shahrara, S., Huang, Q., Mandelin, A.M., Pope, R.M., 2008. Th-17 cells in rheumatoid arthritis. Arthritis Res. Therapy 10 (4), R93.
Shiba, T., Nishimura, D., Kawazoe, Y., Onodera, Y., Tsutsumi, K., Nakamura, R., Ohshiro, M., 2003. Modulation of mitogenic activity of fibroblast growth factors by inorganic polyphosphate. J. Biol. Chem. 278 (29), 26788–26792.
Shiomi, A., Usui, T., 2015. Pivotal roles of gm-csf in autoimmunity and inflammation. Mediators Inflamm. 2015.
Simó, R., Barbosa-Desongles, A., Lecube, A., Hernandez, C., Selva, D.M., 2012. Potential role of tumor necrosis factor-α in downregulating sex hormone–binding globulin. Diabetes 61 (2), 372–382.
Sophia Fox, A.J., Bedi, A., Rodeo, S.A., 2009. The basic science of articular cartilage: structure, composition, and function. Sports Health 1 (6), 461–468.
Stankovic, A., Slavic, V., Stamenkovic, B., Kamenov, B., Bojanovic, M., Mitrovic, D., 2009. Serum and synovial fluid concentrations of ccl2 (mcp-1) chemokine in patients suffering rheumatoid arthritis and osteoarthritis reflect disease activity.. Bratisl Lek Listy 110 (10), 641–646.
Tang, C., Chen, S., Qian, H., Huang, W., 2012. Interleukin-23: as a drug target for autoimmune inflammatory diseases. Immunology 135 (2), 112–124.
Tanimoto, A., Murata, Y., Wang, K.-Y., Tsutsui, M., Kohno, K., Sasaguri, Y., 2008. Monocyte chemoattractant protein-1 expression is enhanced by granulocyte–macrophage colony-stimulating factor via jak2-stat5 signaling and inhibited by atorvastatin in human monocytic u937 cells. J. Biol. Chem. 283 (8), 4643–4651.
Udalova, I.A., Mantovani, A., Feldmann, M., 2016. Macrophage heterogeneity in the context of rheumatoid arthritis. Nat. Rev. Rheumatol. 12 (8), 472–485.
Urbach, C., Gordon, N.C., Strickland, I., Lowne, D., Joberty-Candotti, C., May, R., Herath, A., Hijnen, D., Thijs, J.L., Bruijnzeel-Koomen, C.A., et al., 2015. Combinatorial screening identifies novel promiscuous matrix metalloproteinase activities that lead to inhibition of the therapeutic target il-13. Chemi. Biol. 22 (11), 1442–1452.
Van Landuyt, K.B., Jones, E.A., McGonagle, D., Luyten, F.P., Lories, R.J., 2010. Flow cytometric characterization of freshly isolated and culture expanded human synovial cell populations in patients with chronic arthritis. Arthritis Res. Therapy 12 (1), R15.
Wishart, D.S., Feunang, Y.D., Guo, A.C., Lo, E.J., Marcu, A., Grant, J.R., Sajed, T., Johnson, D., Li, C., Sayeeda, Z., et al., 2017. Drugbank 5.0: a major update to the drugbank database for 2018. Nucleic Acids Res. 46 (D1), D1074–D1082.
Witten, T., Del Rincon, I., Escalante, A., 2000. Modeling the progression of articular erosion in rheumatoid arthritis (ra): initial mathematical models. Math Comput. Model 31 (2–3), 31–38.
Yoshida, K., Kobayashi, K., Yamagata, N., Iwabuchi, H., Katsura, T., Sugihara, S., Negishi, M., Ide, H., Mori, Y., Takahashi, T., 1992. Inflammatory cytokines and enzymes in synovial fluid of patients with rheumatoid arthritis and other arthritides. Int. Arch. Allergy Immunol. 98 (4), 286–292.
Yoshihara, Y., Nakamura, H., Obata, K., Yamada, H., Hayakawa, T., Fujikawa, K., Okada, Y., 2000. Matrix metalloproteinases and tissue inhibitors of metalloproteinases in synovial fluids from patients with rheumatoid arthritis or osteoarthritis. Ann. Rheum. Dis. 59 (6), 455–461.
Young, M., Carroad, P., Bell, R., 1980. Estimation of diffusion coefficients of proteins. Biotechnol. Bioeng. 22 (5), 947–955.
Yuan, F.-L., Li, X., Lu, W.-G., Sun, J.-M., Jiang, D.-L., Xu, R.-S., 2013. Epidermal growth factor receptor (egfr) as a therapeutic target in rheumatoid arthritis. Clin. Rheumatol. 32 (3), 289–292.